Example 2: experiments at LHC

Peter Križan

University of Ljubljana and J. Stefan Institute

University of Ljubljana

"Jožef Stefan" Institute

Contents

General purpose experiments: ATLAS and CMS

Heavy ion collisions: ALICE

General purpose experiments: ATLAS and CMS

Goals:

- Find Higgs
- Search for new (heavy) particles

Zakaj imajo delci maso: Higgsov bozon

Škotski fizik Peter Higgs in belgijski fizik Francois Englert, 1964:
Maso delcev lahko pojasnimo, če predpostavimo, da je prostor napolnjen s poljem – Higgsovim poljem

Elektromagnetno polje → nabit delec (e^-) občuti silo
velikost sile odvisna od velikosti električnega naboja

Higgsovo polje → delci imajo maso

velikost mase odvisna od velikosti „Higgsovega naboja“

→

Higgsov bozon

Škotski fizik Peter Higgs in belgijski fizik Francois Englert, 1964:
Maso delcev lahko pojasnimo, če predpostavimo, da je prostor napolnjen s poljem, seveda – Higgsovim poljem

Elektromagnetno polje → nabit delec (e^-) občuti silo

velikost sile odvisna od velikosti električnega naboja

Higgsovo polje → delci imajo maso

velikost mase odvisna od velikosti „Higgsovega naboja“

elektromagnetno polje ima svoje delce – fotone
Higgsovo polje ima svoje delce – Higgsove bozone

Generic LHC Detector for all Particles

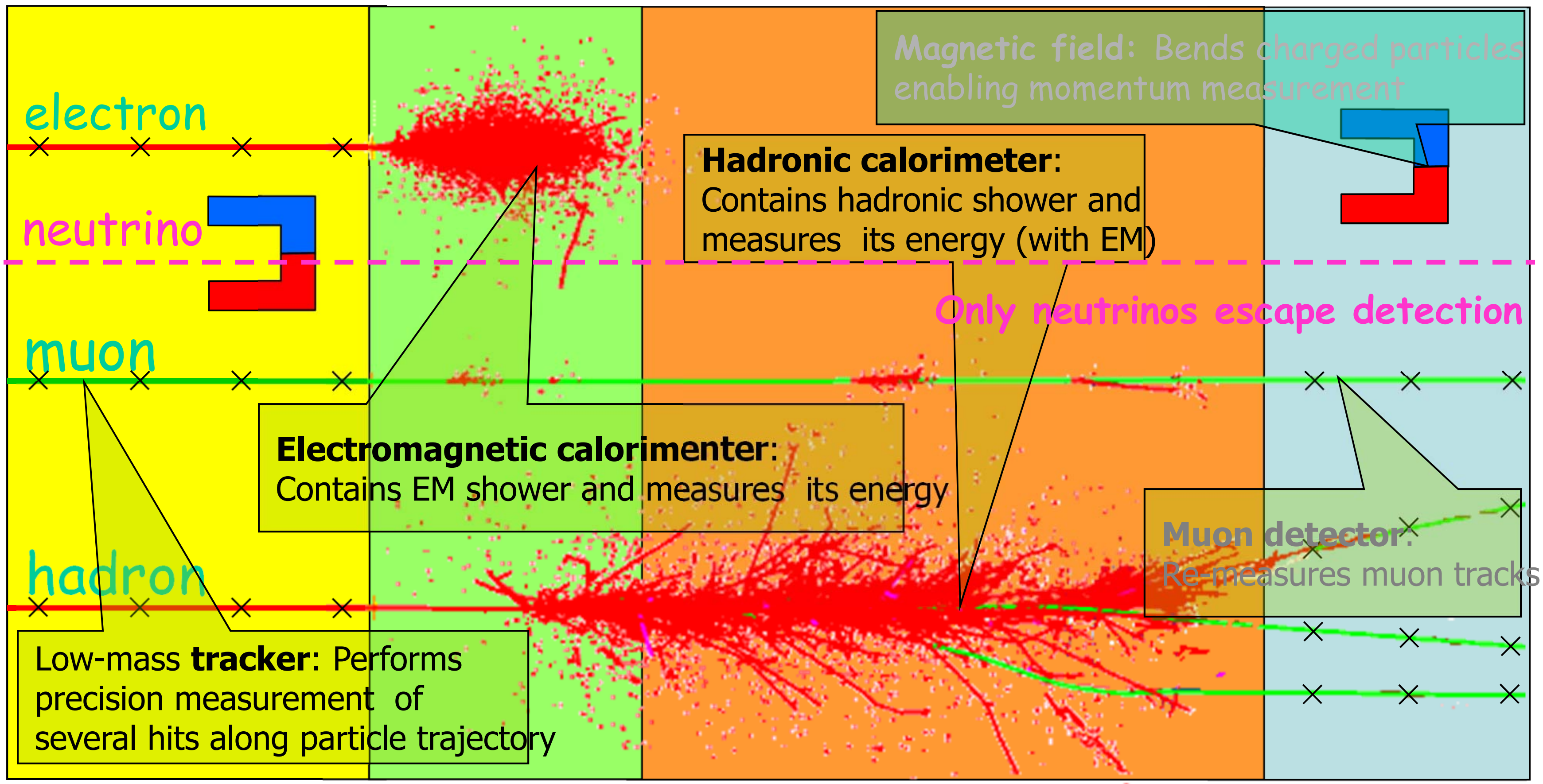

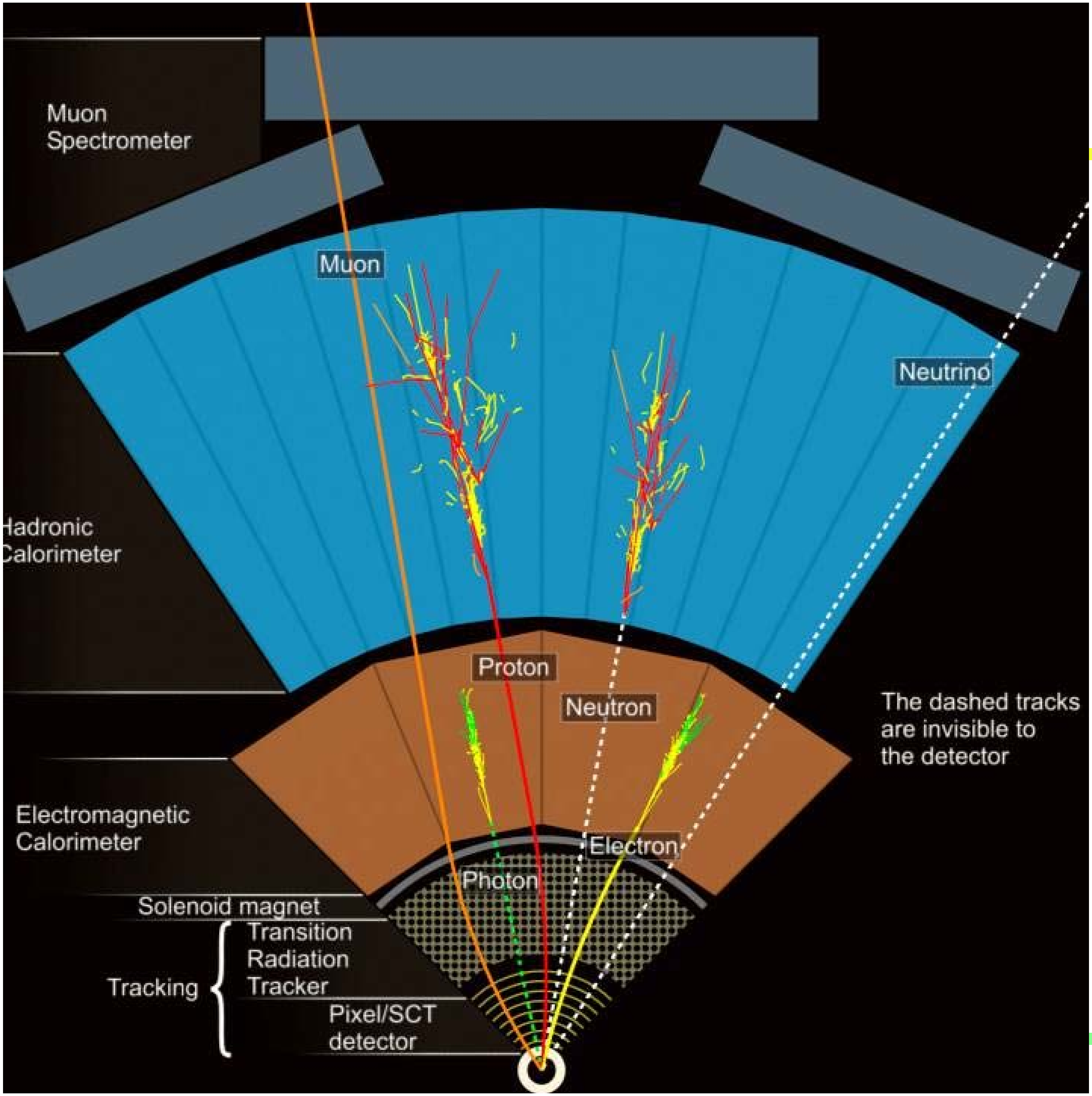
Muon Spectrometer
Muon
Neutrino
Hadronic Calorimeter
Proton
Neutron
The dashed tracks are invisible to the detector
Electromagnetic Calorimeter
Electron
Photon
Solenoid magnet
Transition Radiation Tracker
Tracking
Pixel/SCT detector

Muon spectrum -ATLAS

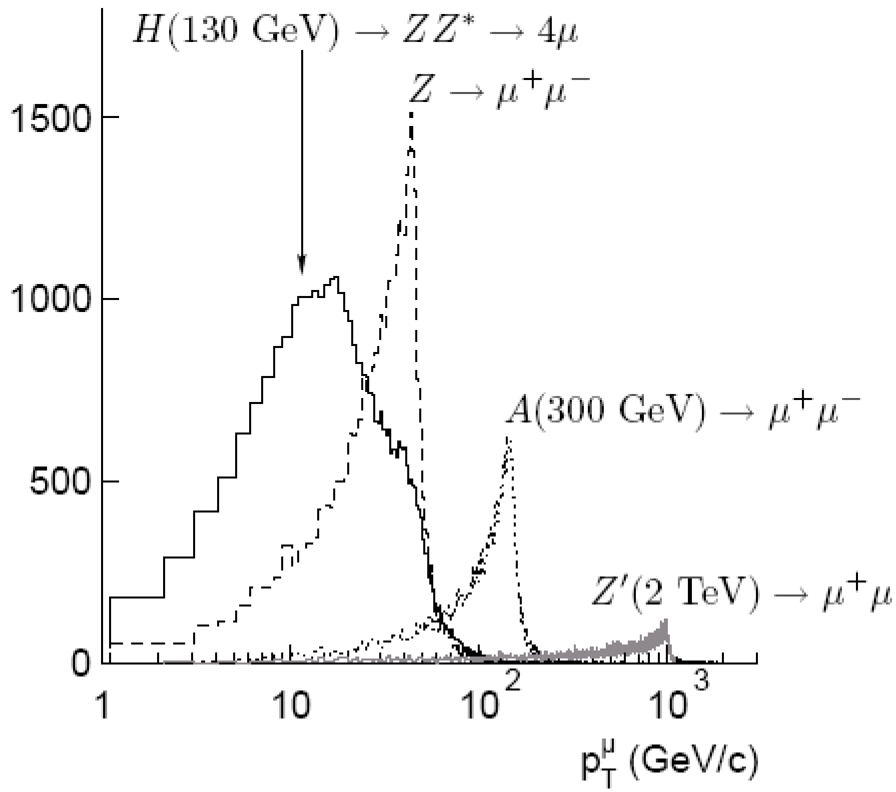

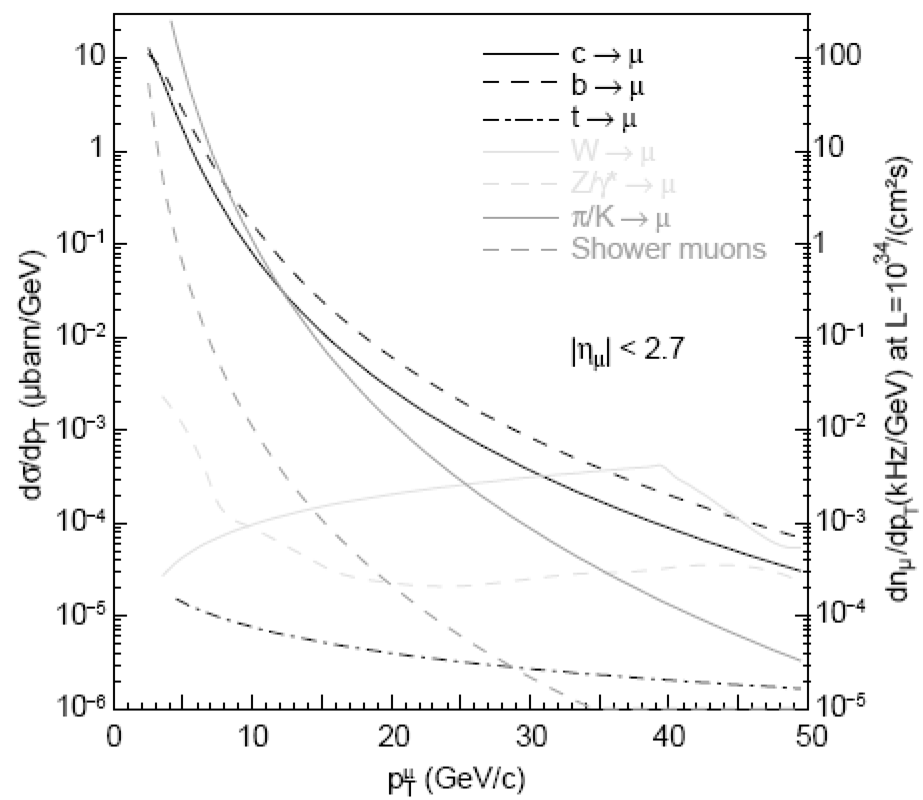

From raw data to summary data

momentum measurement

Example of momentum determination:

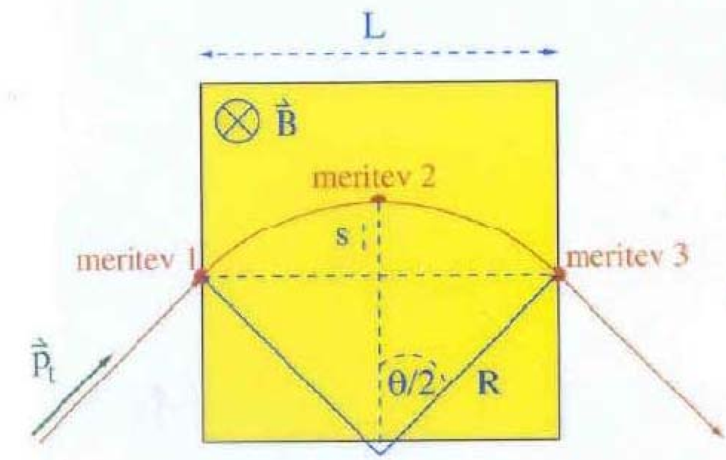

$$p_t = q\,B\,R \Rightarrow R = \frac{p_t}{qB}$$

$$\sin\frac{\theta}{2} \approx \frac{\theta}{2} = \frac{L}{2R}$$

$$\cos\frac{\theta}{2} = \frac{R-s}{R} \Rightarrow s \approx R\frac{\theta^2}{8}$$

$$s = \frac{B\;L^2\;q}{8p_t}$$

if s determined by
3 measurement points:

$$s = x_2 - \frac{x_1 + x_3}{2}$$

$$\frac{\sigma(p_t)}{p_t} = \frac{\sigma(s)}{s} = \frac{\sqrt{\frac{3}{2}}\sigma(x)8p_t}{BL^2q}$$

for N measurement points:

$$\frac{\sigma_{p_T}}{p_T} = \frac{\sigma_x p_T}{eBL^2}\sqrt{\frac{720}{N+4}}$$

eB = 0.3 (B/T) (1/m) GeV/c

From raw data to summary data
momentum measurement

Multiple scattering:

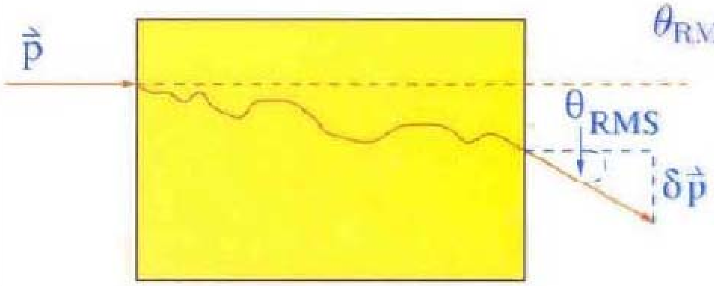

$$\theta_{RMS} \approx \frac{13.6\text{MeV}}{cp\beta}\sqrt{\frac{L}{X_0}}\left[1 + 0.038\ln\frac{L}{X_0}\right]$$

$$\delta p = p\sin\theta_{RMS}$$

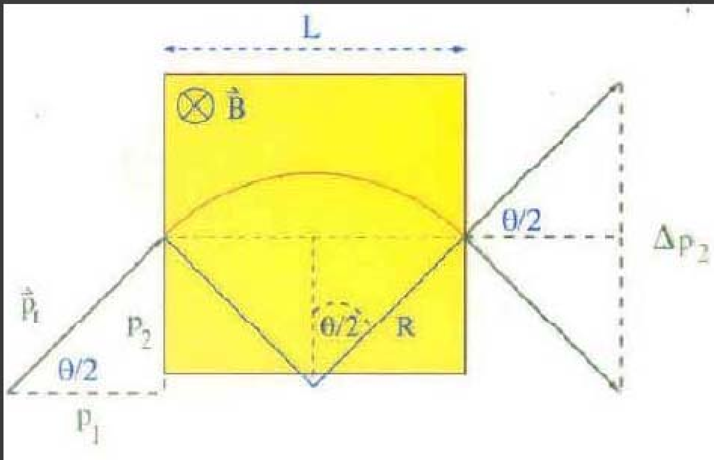

$$\Delta p_2 = 2p_t\sin\frac{\theta}{2} \approx p_t\theta$$

$$\frac{\sigma(p_t)}{p_t} = \frac{\sigma(\Delta p_2)}{\Delta p_2}$$

$$\frac{\sigma(p_t)}{p_t} \approx \frac{p_t\sin\theta_{RMS}}{p_t\theta} \approx \frac{\theta_{RMS}}{\theta}$$

$$\frac{\sigma(p_t)}{p_t} \approx \frac{13.6\ \text{MeV}}{qB\sqrt{LX_0}}$$

eB = 0.3 (B/T) (1/m) GeV/c

Tracking system of the inner detector

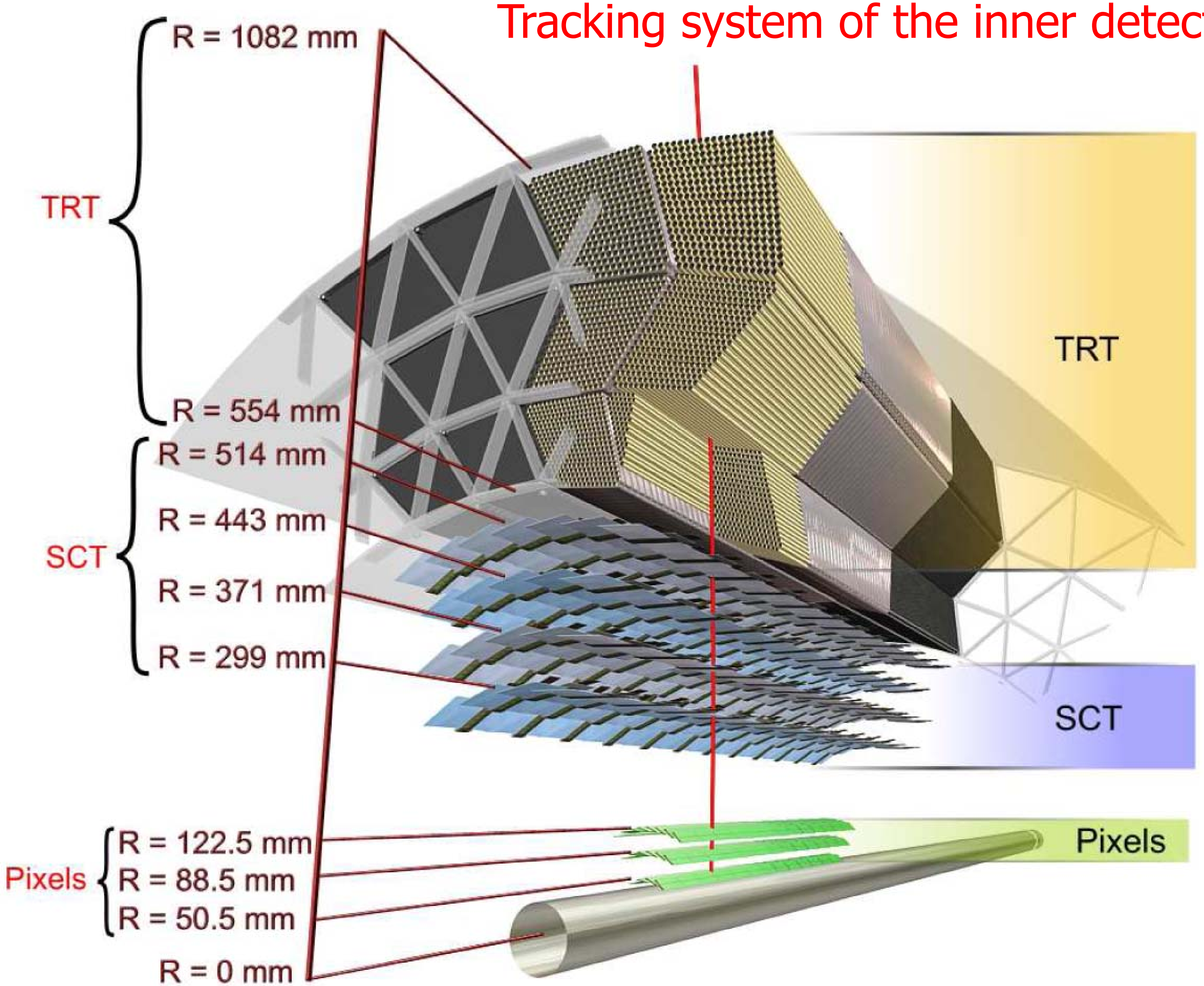

ına

What kind of momentum resolution do we need?

Reminder: example X → $\mu^- \mu^+$

$M^2c^4 = (E_1 + E_2)^2 - (p_1 + p_2)^2 \rightarrow M^2c^4 = 2\, p_1\, p_2\, (1 - \cos\Theta_{12})$

The X peak should be narrow to minimize the contribution of random coincidences ('combinatorial background')

The required resolution in Mc^2: about 1 GeV at 30 GeV.

What is the corresponding momentum resolution?

For simplicity assume X is at rest → $\Theta_{12}=180^0$, $p_1=p_2=p=15$ GeV/c, $Mc^2=2pc$
→$\sigma(Mc^2) = 2\,\sigma(pc)$ at p=15 GeV/c

→ $\sigma(p)/p = 1$ GeV/2/15GeV = 3%

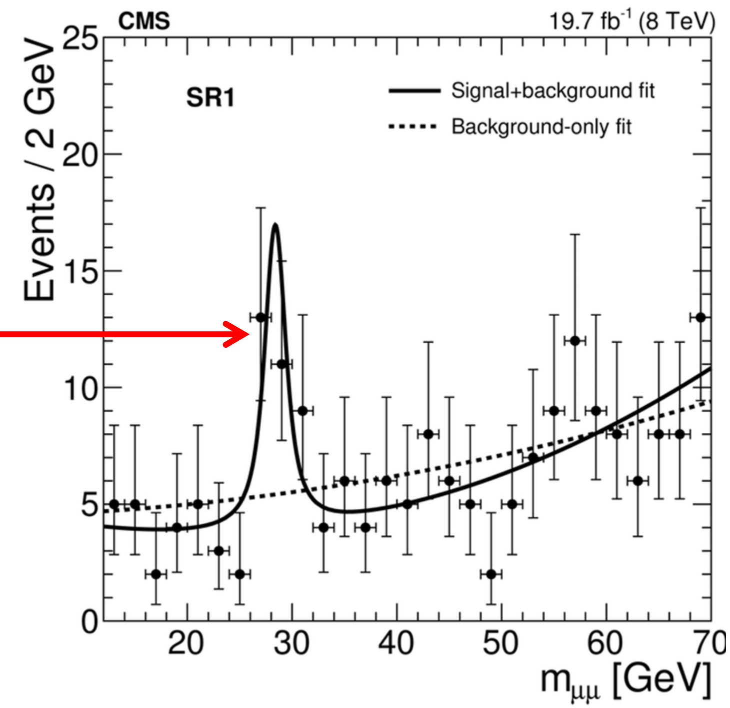

CMS could-be-particle (porobably statistical fluctuation…)

Momentum resolution

$$\frac{\sigma_{p_T}}{p_T} = \frac{\sigma_x p_T}{eBL^2}\sqrt{\frac{720}{N+4}}$$

$$\frac{\sigma_{p_T}}{p_T} = \frac{13.6MeV}{eB\sqrt{LX_0}}$$

$$\frac{\sigma_{p_T}}{p_T} = p_T \frac{0.1\times 10^{-3} m}{0.3(GeV/m)\times 2 \times 1m^2}\sqrt{\frac{720}{54}} = p_T \times 0.0006$$

eB = 0.3 (B/T) (1/m) GeV/c

For B=2T, L = 1m, σ_x = 0.1 mm

For p_T = 1 GeV: σ_{pT}/p_T = 0.06%

For p_T = 10 GeV: σ_{pT}/p_T = 0.6%

For p_T = 100 GeV: σ_{pT}/p_T = 6%

How to improve high momentum resolution?

- Better resolution: wire chamber → silicon strip detector (full CMS tracker, partly ATLAS)
- Higher field: CMS B=4T
- Longer lever arm for muons: additional tracking in the magnetic muon system (ATLAS)

Momentum measurement for very high energy muons - example ATLAS

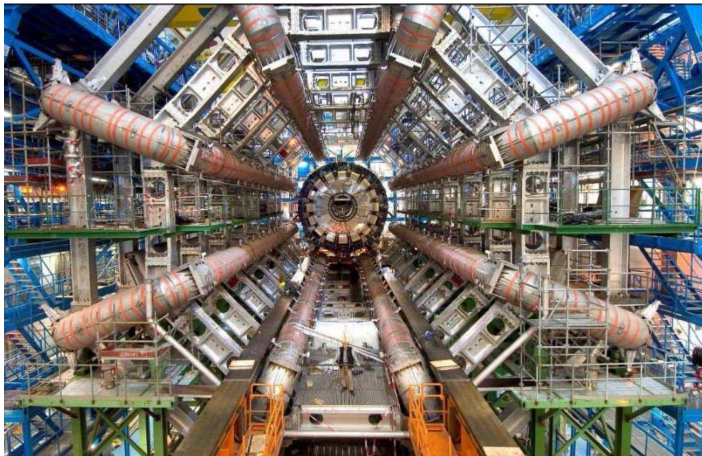

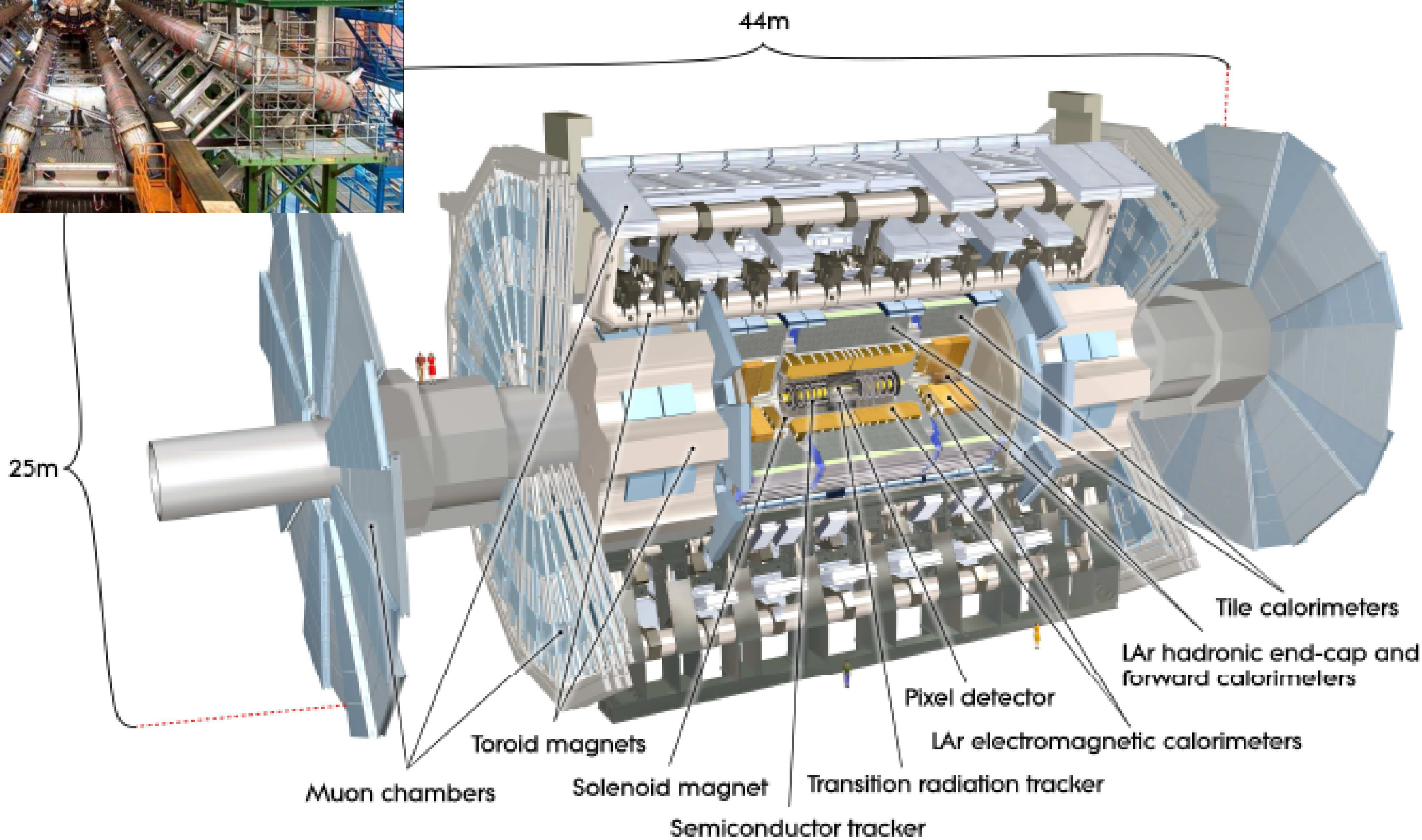

Tipične številke

ATLAS B = 2T

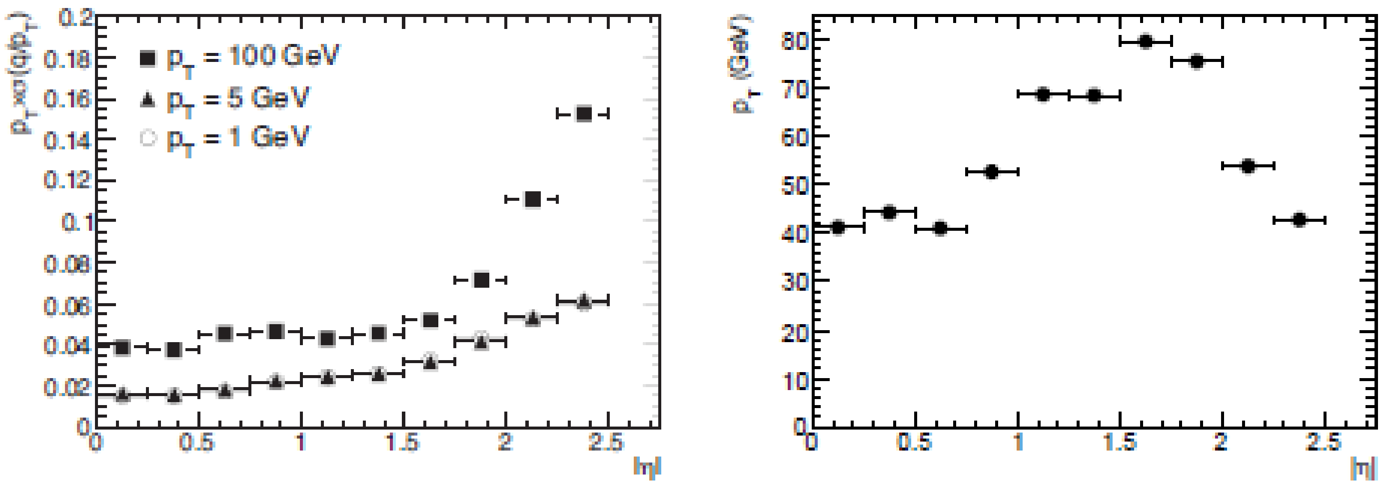

Figure 10.8: Relative transverse momentum resolution (left) as a function of $|\eta|$ for muons with p_T = 1 GeV (open circles), 5 GeV (full triangles) and 100 GeV (full squares). Transverse momentum, at which the multiple-scattering contribution equals the intrinsic resolution, as a function of $|\eta|$ (right).

$\eta = -\ln \mathrm{tg}\, \theta/2$

Identification of charged particles

Particles are identified by their mass or by the way they interact.

Determination of mass: from the relation between momentum and velocity, $p=\gamma mv$ (p is known - radius of curvature in magnetic field)

→Measure velocity by:

- time of flight
- ionisation losses dE/dx
- Cherenkov photon angle (and/or yield)
- transition radiation

Mainly used for the identification of hadrons.

Identification through interaction: electrons and muons

→calorimeters, muon systems

Transition radiation

E.M. radiation emitted by a charged particle at the boundary of two media with different refractive indices

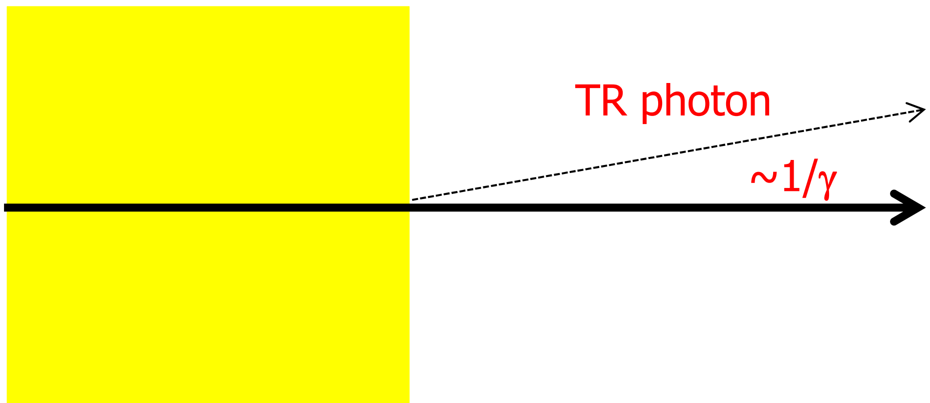

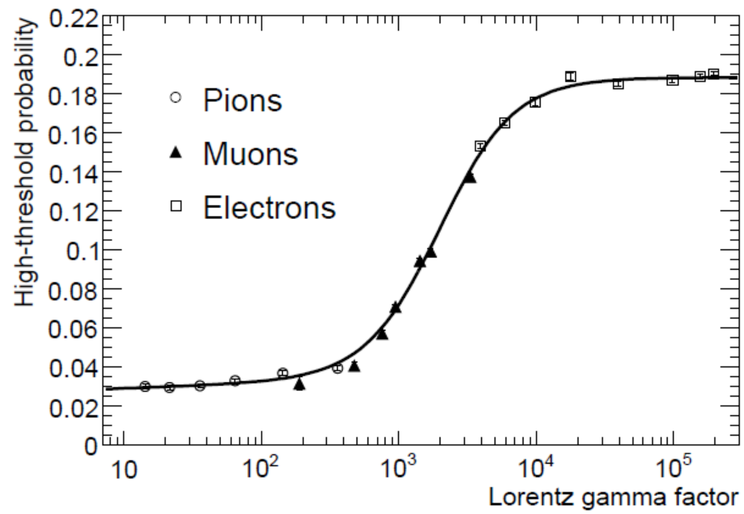

Emission rate depends on γ (Lorentz factor): becomes important at $\gamma \sim 1000$

- Electrons at 0.5 GeV
- Pions above 140 GeV

Emission probability per boundary $\sim\alpha = 1/137$

Emission angle $\sim 1/\gamma$

Typical photon energy: ~10 keV → X rays

Transition radiation - detection

Emission probability per boundary ~α = 1/137

→ Need many boundaries

- Stacks of thin foils or
- Porous materials – foam with many boundaries of individual ‘bubbles’

Typical photon energy: ~10 keV → X rays

→ Need a wire chamber with a high Z gas (Xe) in the gas mixture

Emission angle ~1/γ

→ Hits from TR photons along the charged particle direction

- Separation of X ray hits (high energy deposit on one place) against ionisation losses (spread out along the track)
- Two thresholds: lower for ionisation losses, higher for X ray detection

Transition radiation - detection

→ Hits from TR photons along the charged particle direction

- Separation of X ray hits (high energy deposit on one place) against ionisation losses (spread out along the track)
- Two thresholds: lower for ionisation losses, higher for X ray detection

  - Small circles: low threshold (ionisation)
  - Big circles: high threshold (X ray detection)

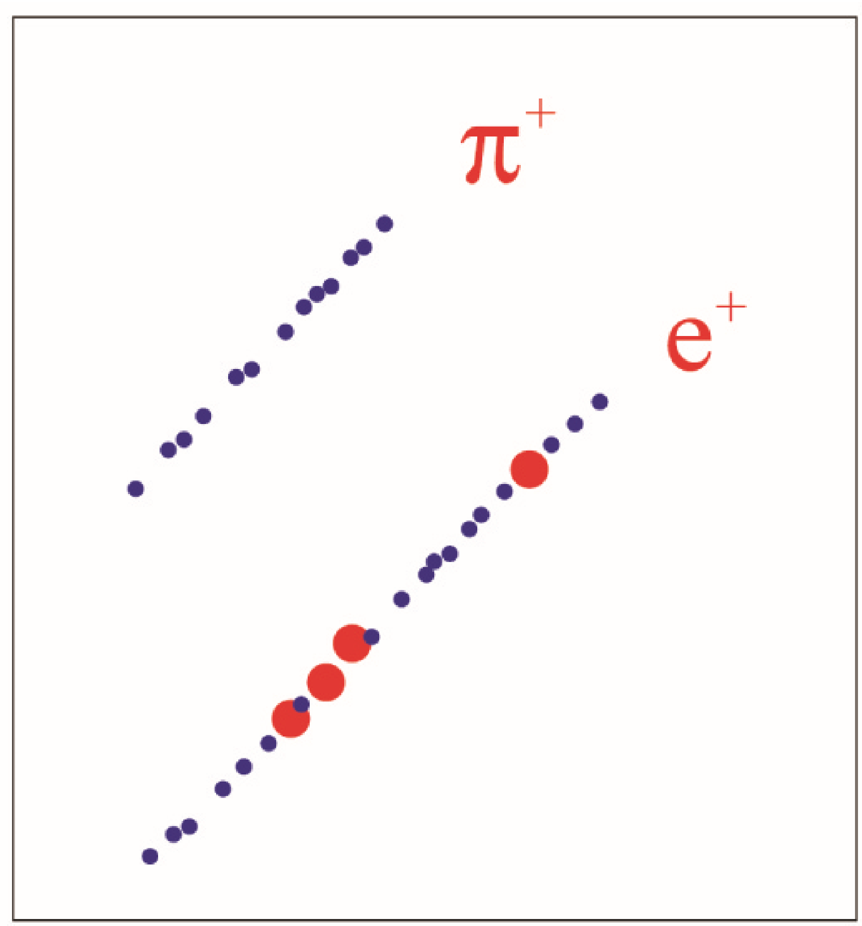

Transition radiation detectors

Example:

Radiator: organic foam between the detector tubes (straws made of capton foil)

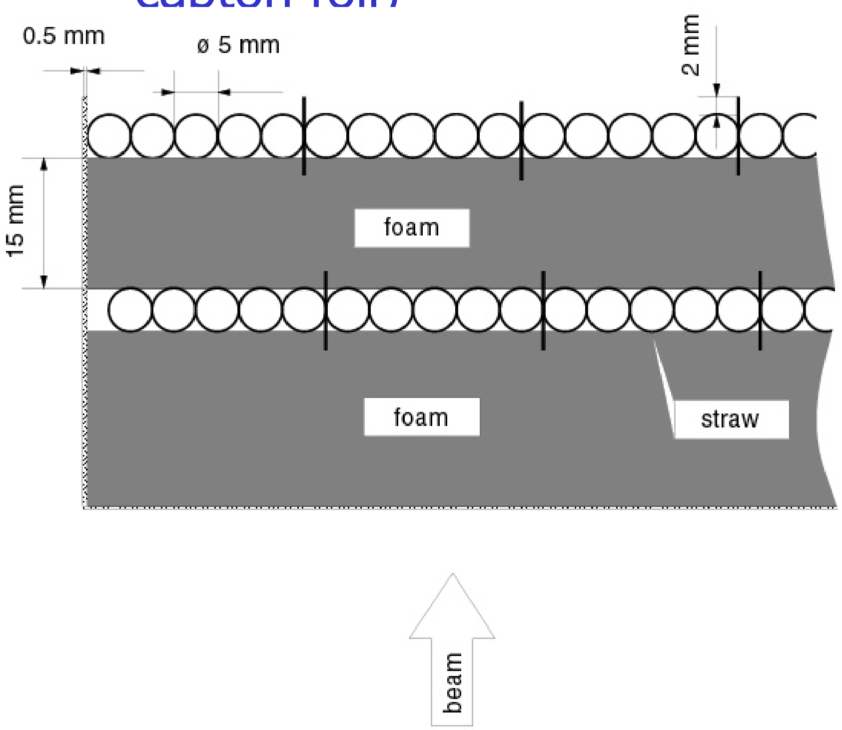

Performance: pion efficiency (fake prob.) vs electron efficiency

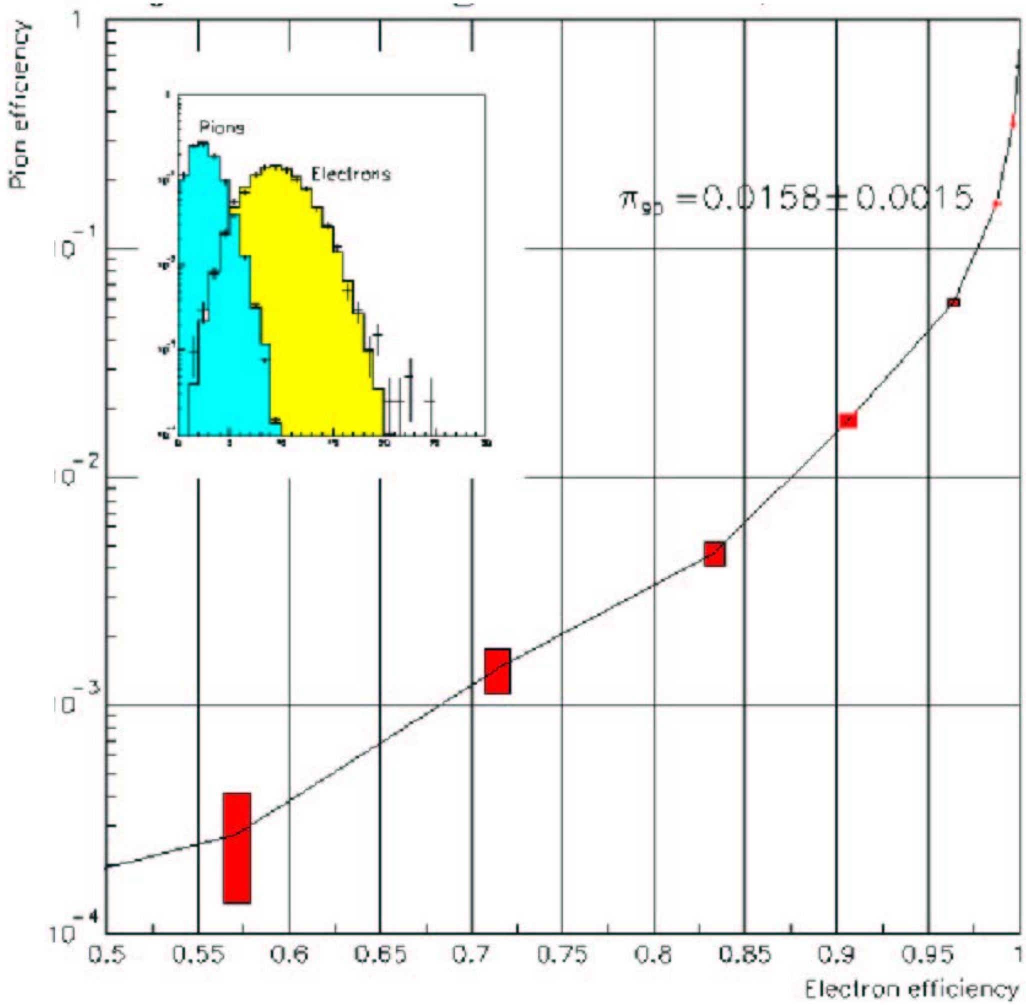

Transition radiation detector in ATLAS: combination of a tracker and a transition radiation detector

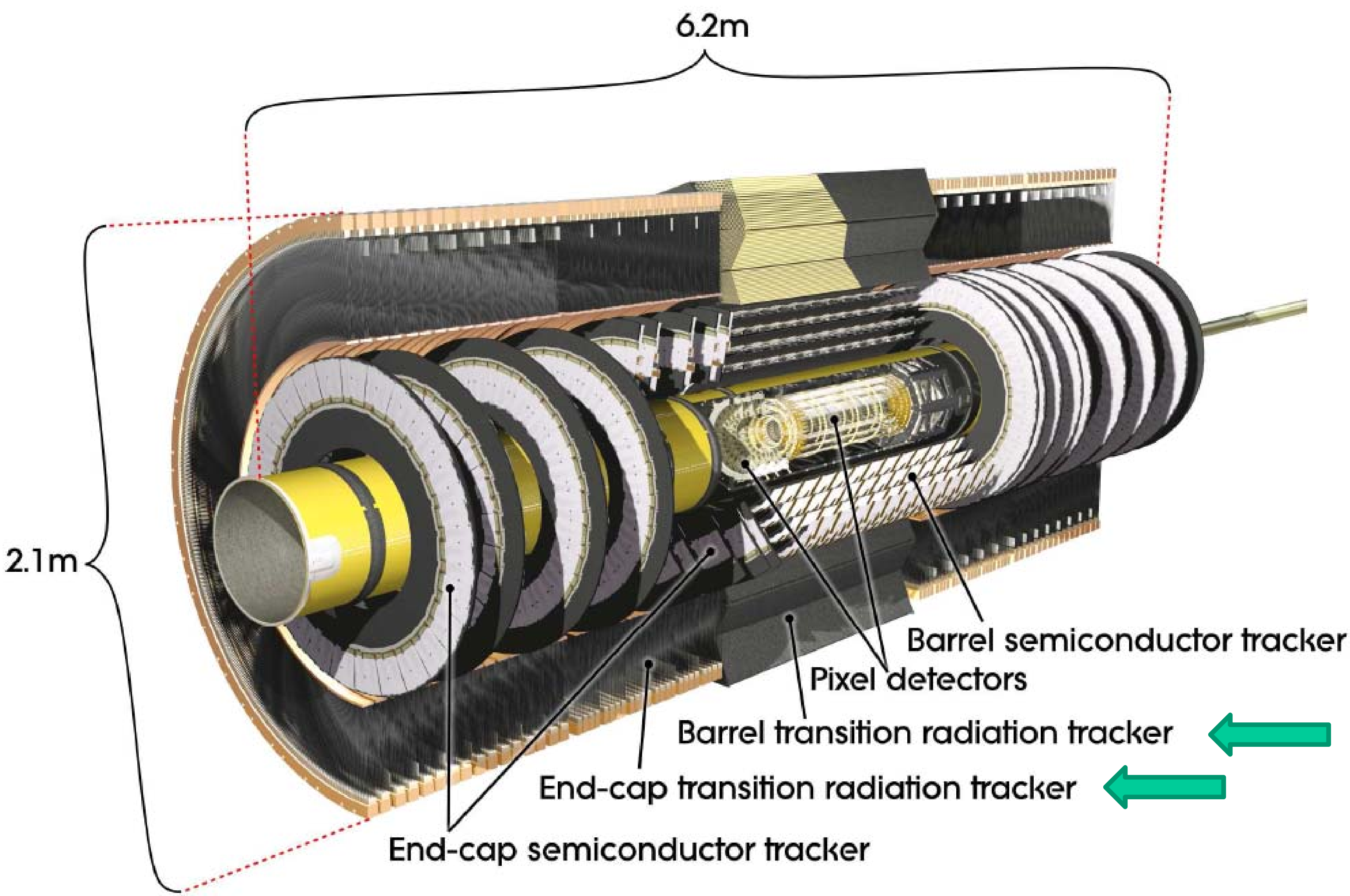

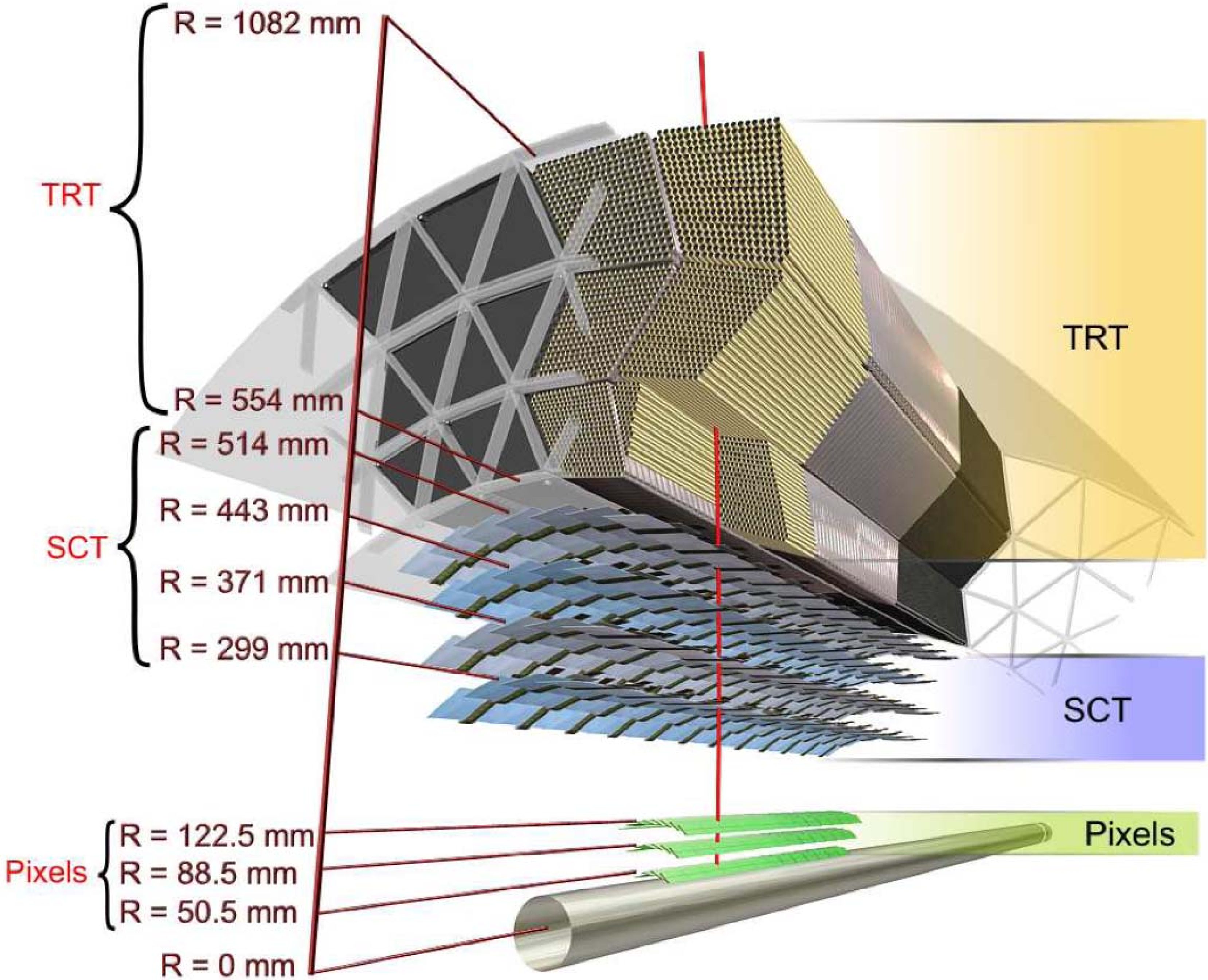
R = 1082 mm
TRT
R = 554 mm
R = 514 mm
R = 443 mm
SCT
R = 371 mm
R = 299 mm
TRT
SCT
R = 122.5 mm
Pixels
R = 88.5 mm
R = 50.5 mm
R = 0 mm
Pixels

ına

ATLAS TRT

Radiator: 3mm thick layers made of polypropylene-polyethylene fibers with ~19 micron diameter, density: 0.06 g/cm^3

Straw tubes: 4mm diameter with 31 micron diameter anode wires, gas: 70% Xe, 27% CO_2, 3% O_2.

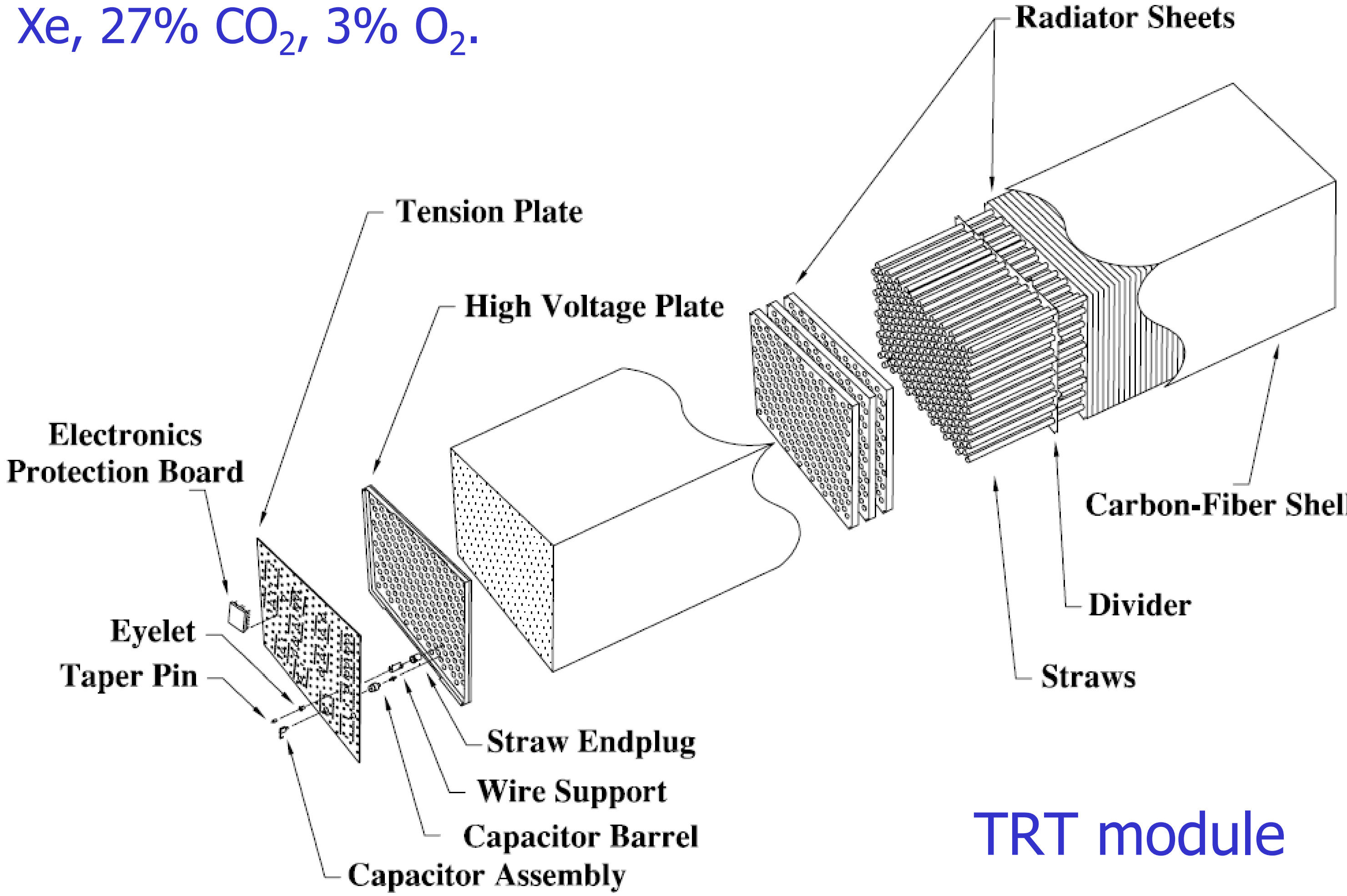

TRT module

TRT: pion-electron separation

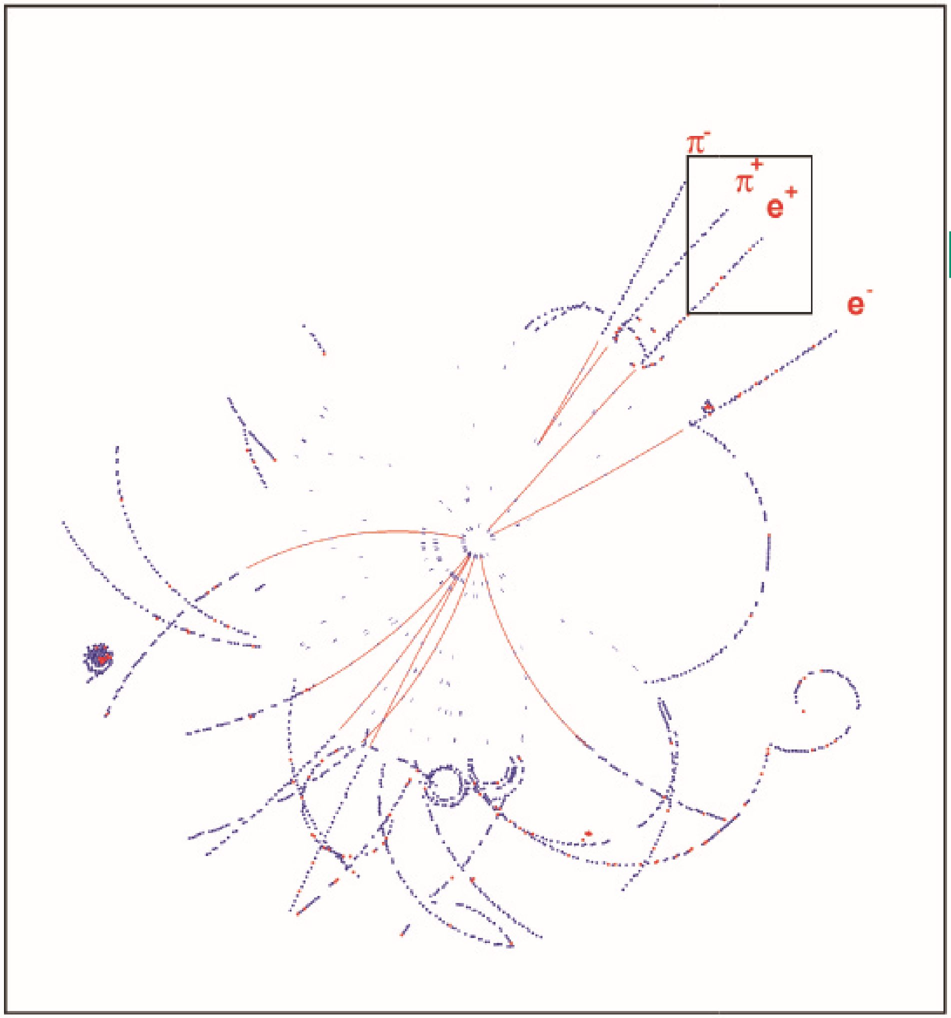

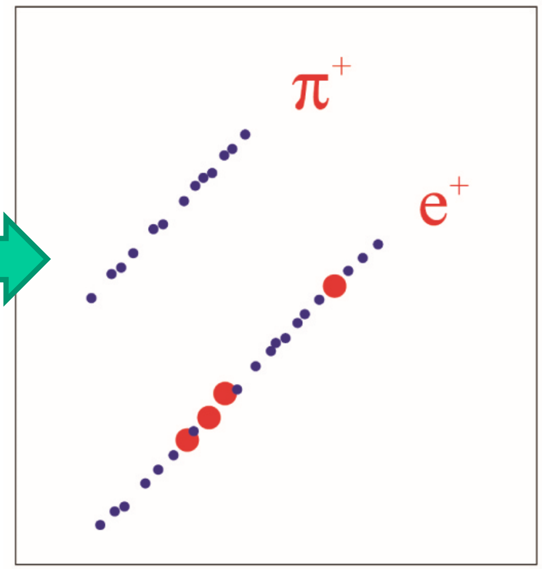

Expected π fake probability at 90% e efficiency

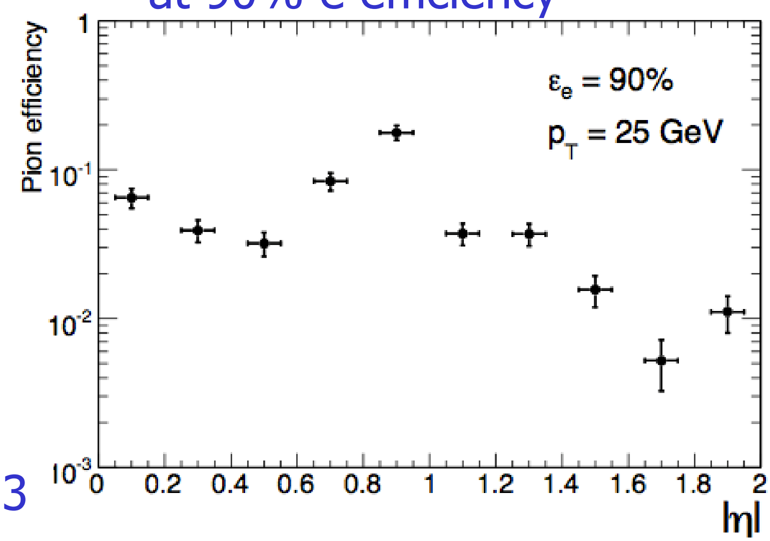

→ JINST 3 (2008) S08003

TRT performance in 2010 data

e/pion separation: high threshold hit probability per straw

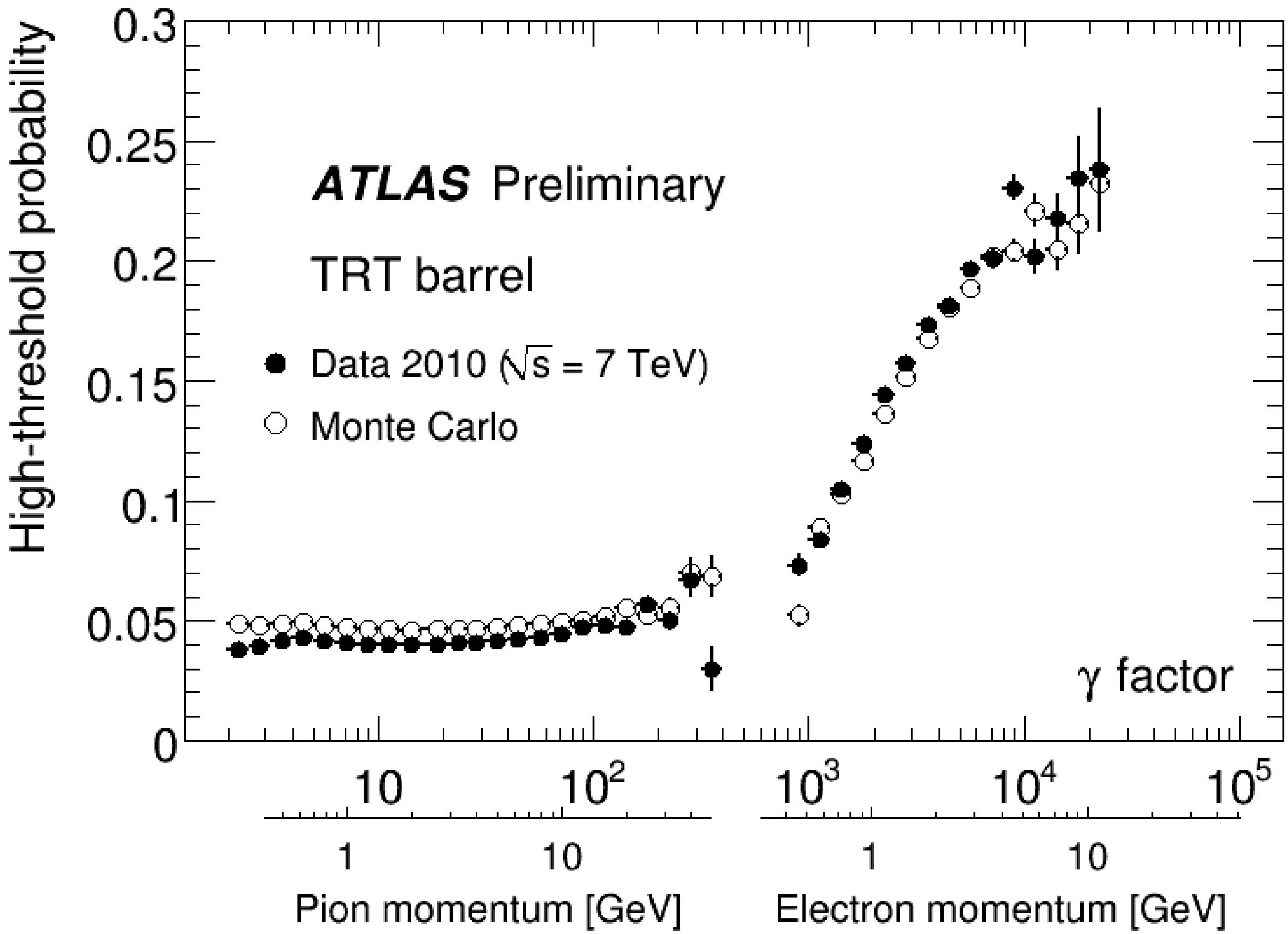

Additional feature of TRT: identification with a dE/dx measurement

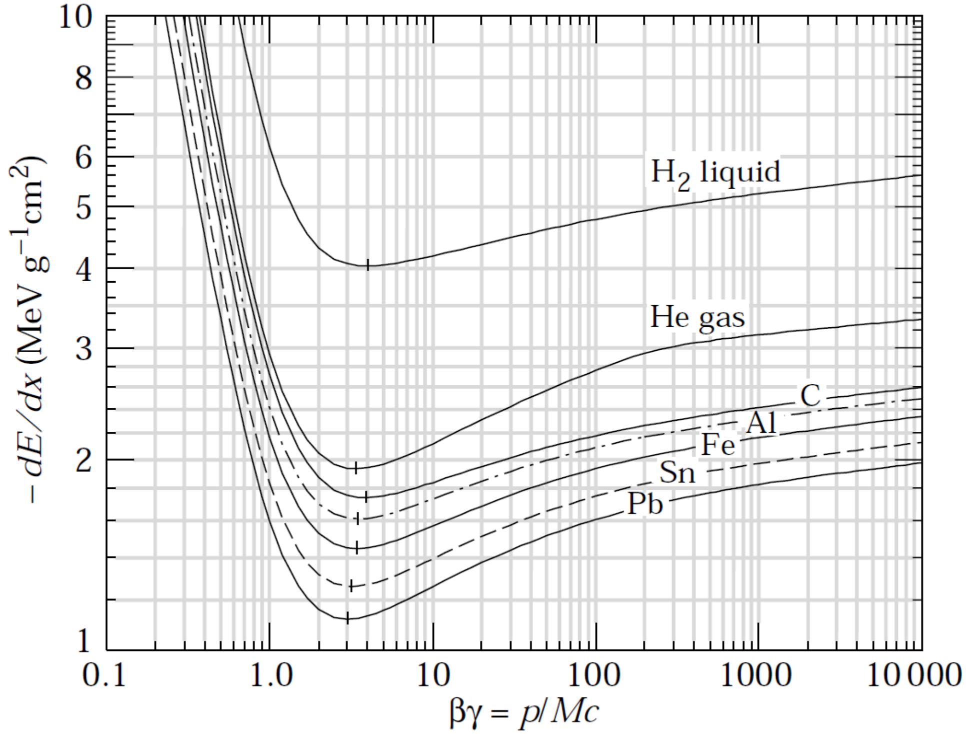

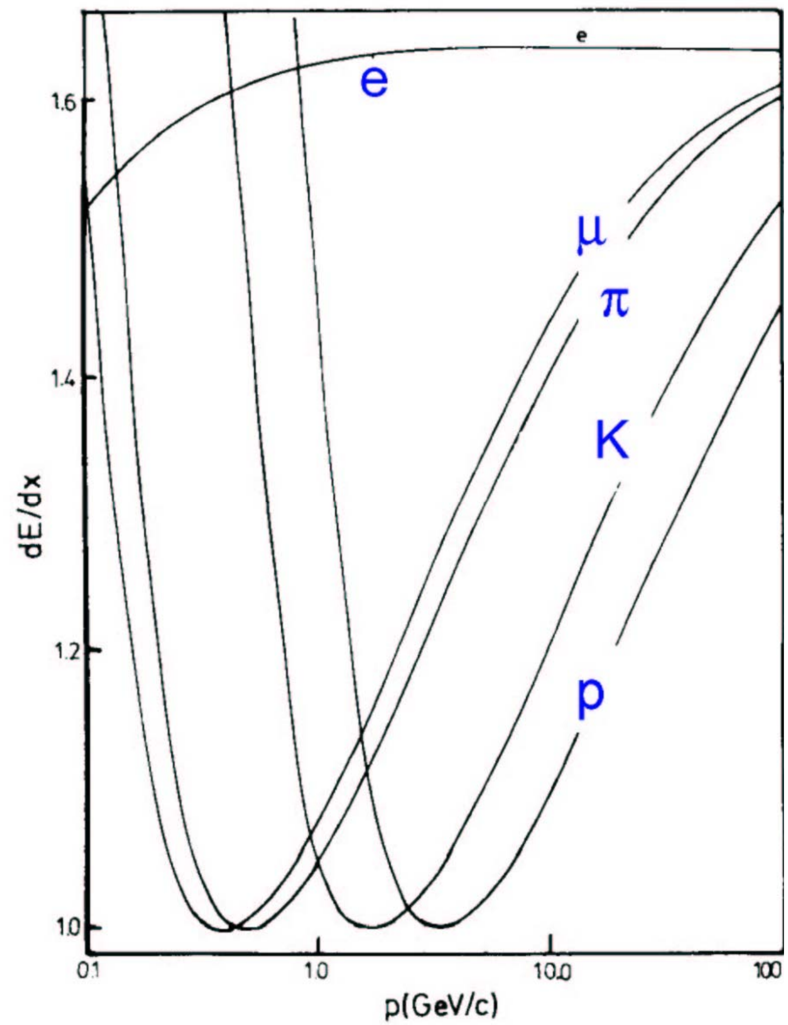

dE/dx is a function of velocity β

For particles with different mass the Bethe-Bloch curve gets displaced if plotted as a function of p

For good separation: resolution should be ~5%

Time-over-Threshold (ToT): dE/dx in ATLAS TRT

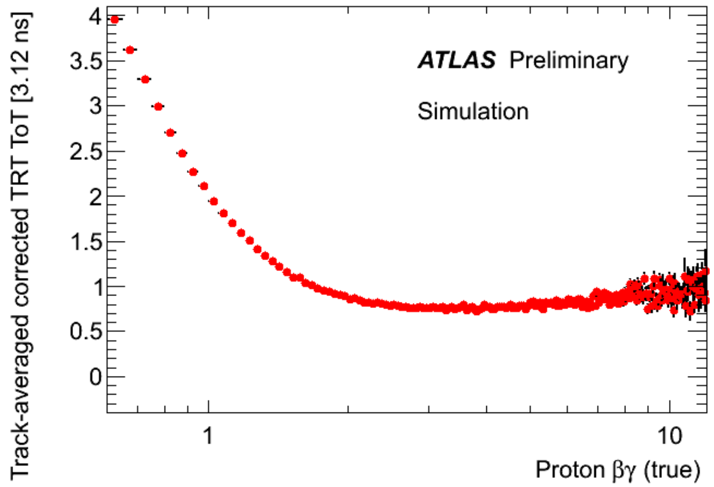

The relation between the track ToT measurement and the track βγ, obtained from MC studies.

2010 data: The track-averaged ToT distribution as a function of the track momentum.

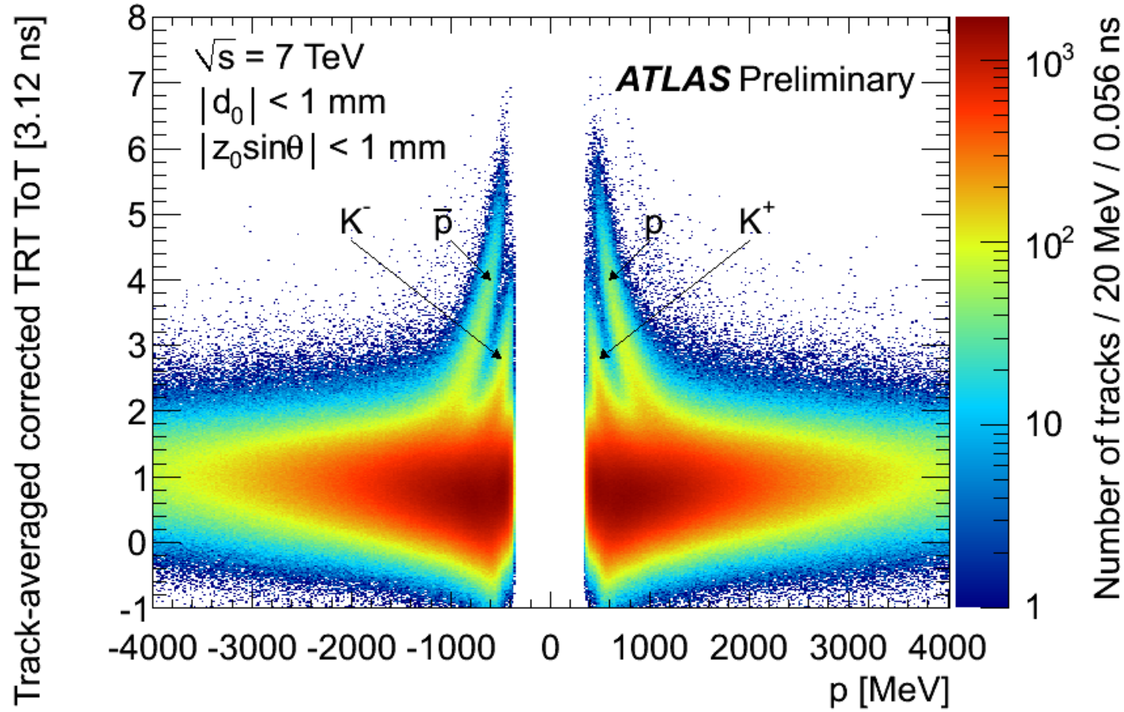

Identification of muons at LHC - example ATLAS

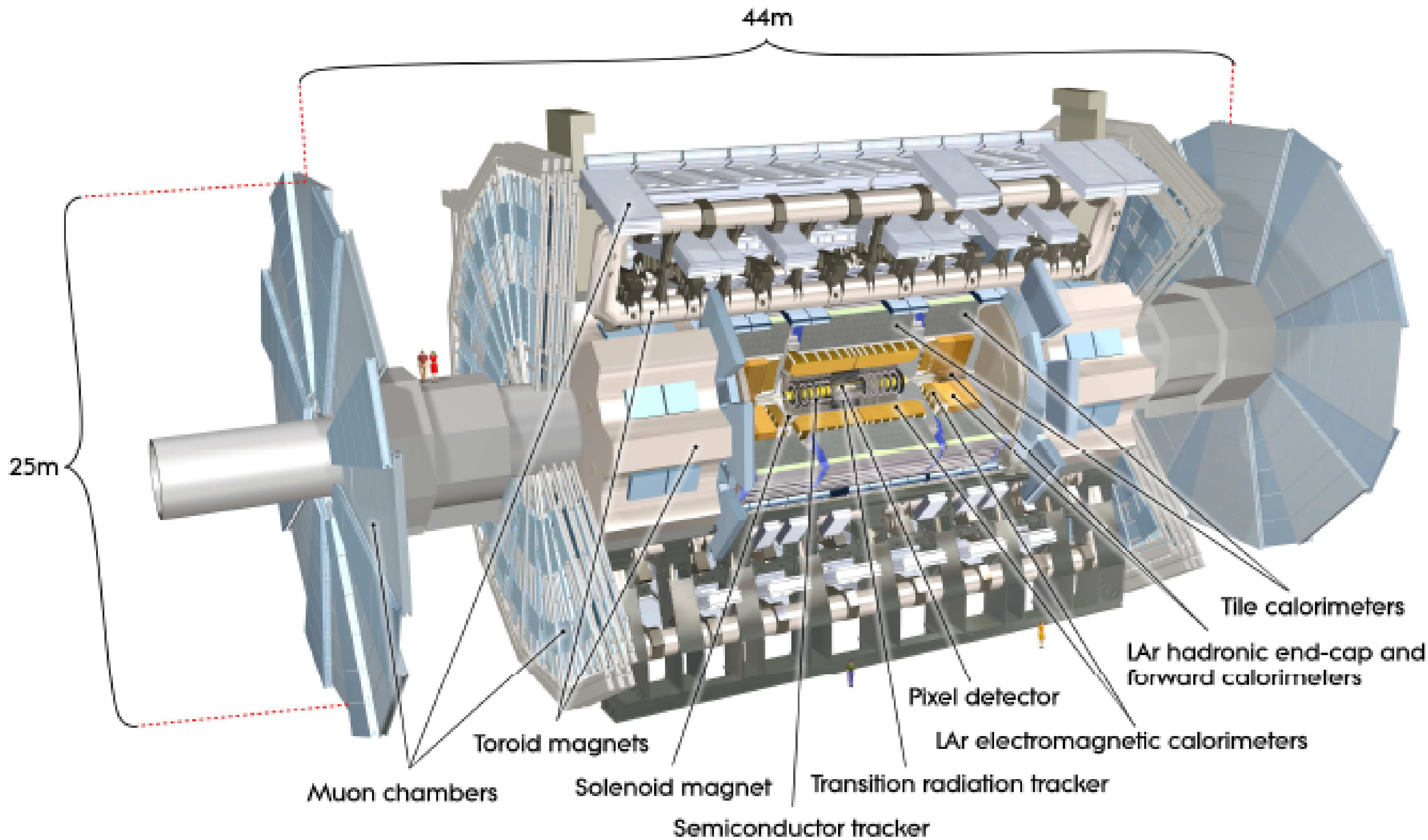

Muon ID

Separate muons from hadrons (pions and kaons): exploit the fact that muons interact only electromag., while hadrons interact strongly → need a few interaction lengths to stop hadrons

Interaction lengths = about 10x radiation length in iron, 20x in CsI.

A particle is identified as a muon if it penetrates the material.

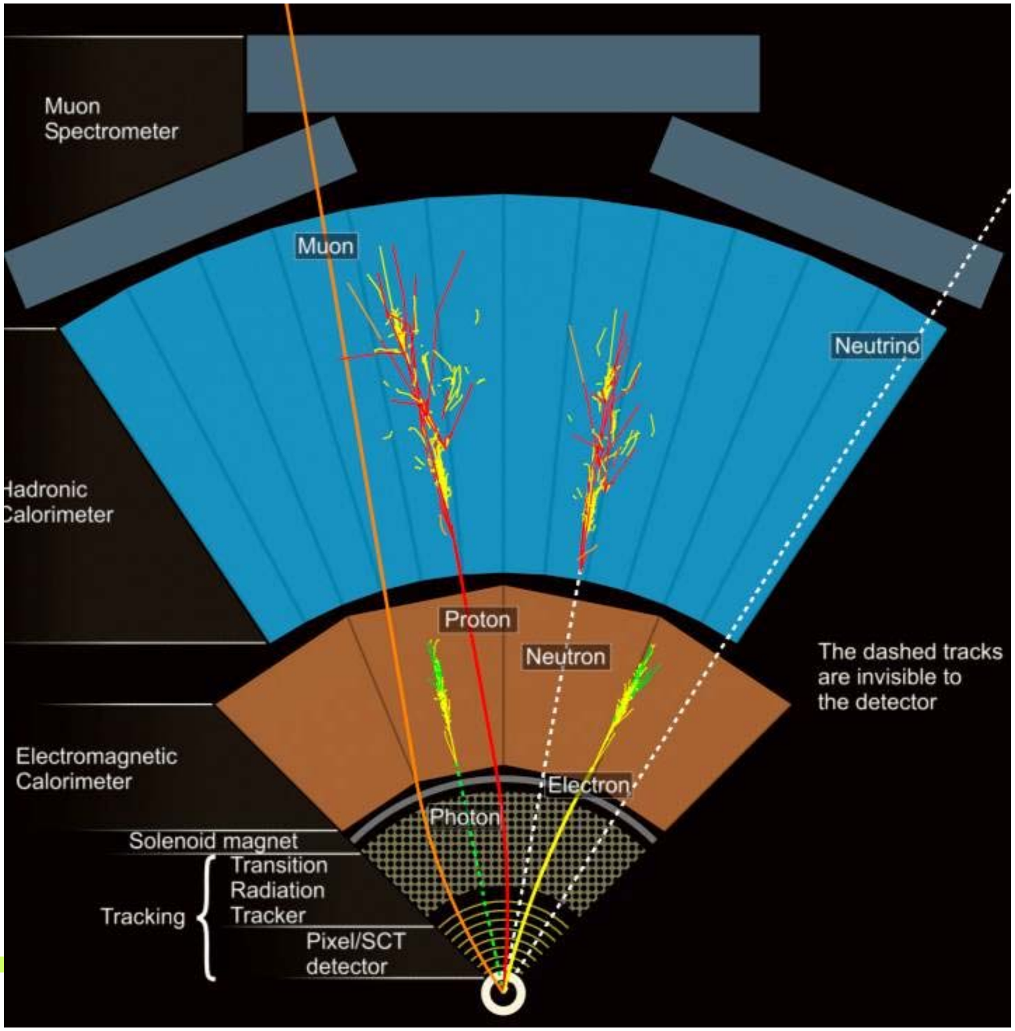

Identification of muons in ATLAS

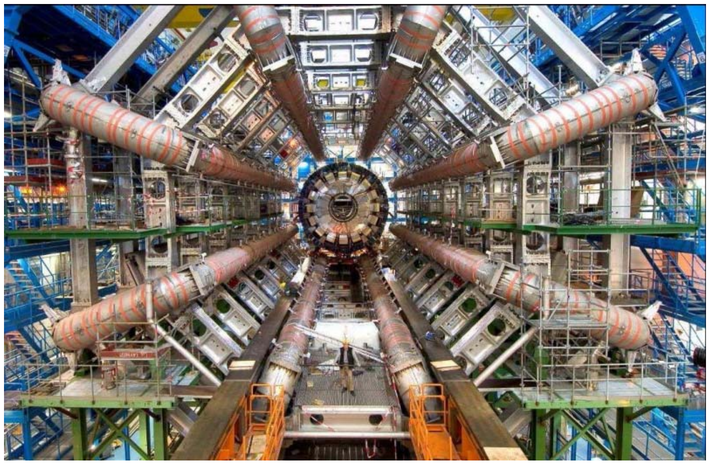

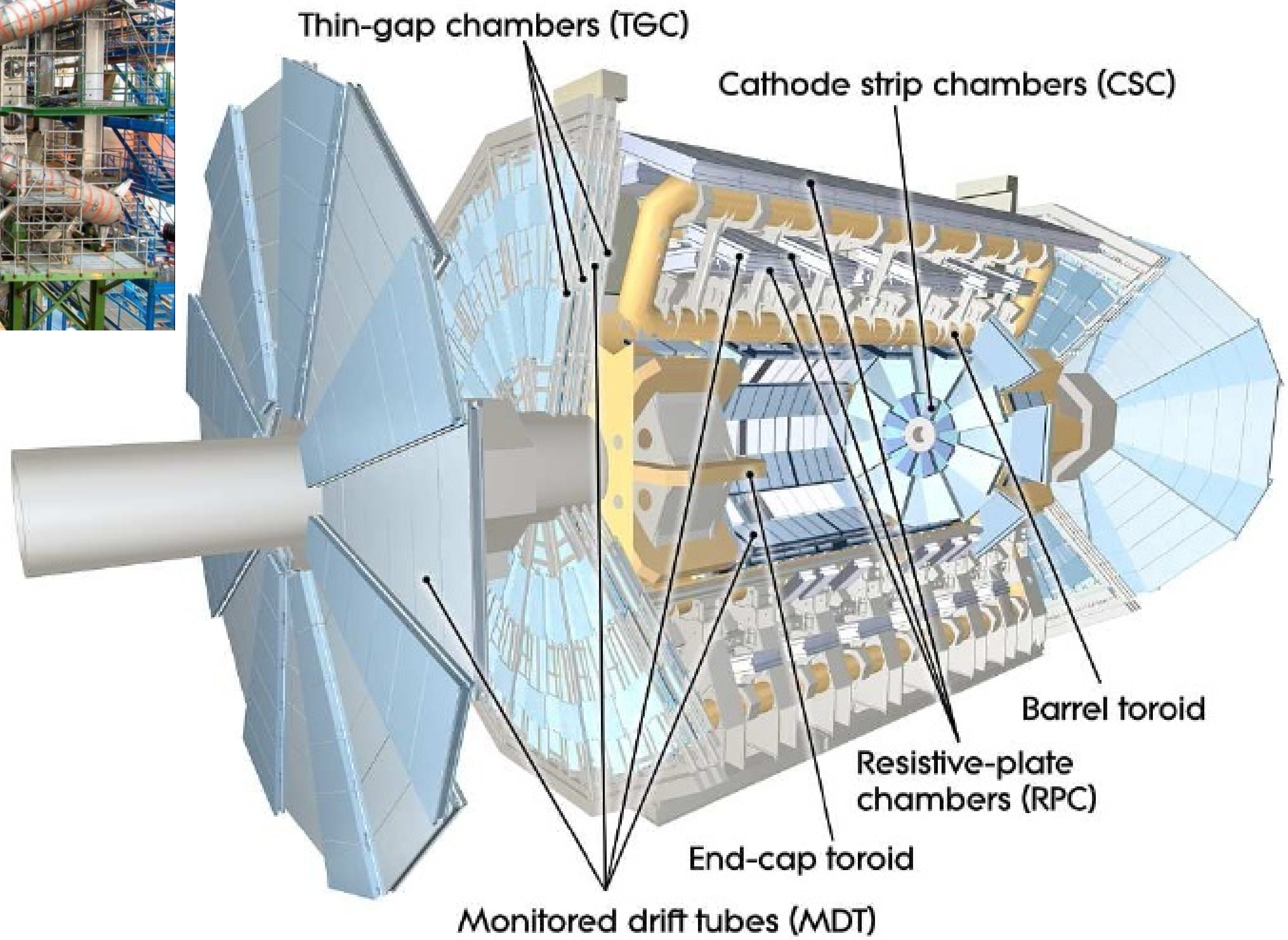

- Identify muons
- Measure their momentum

Muon spectrum

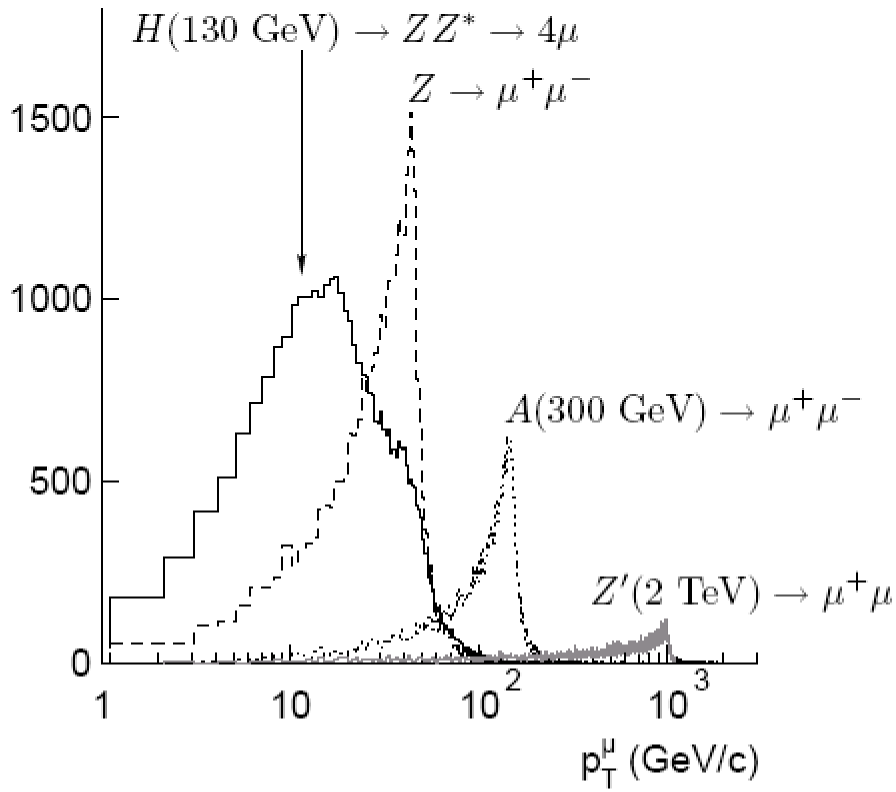

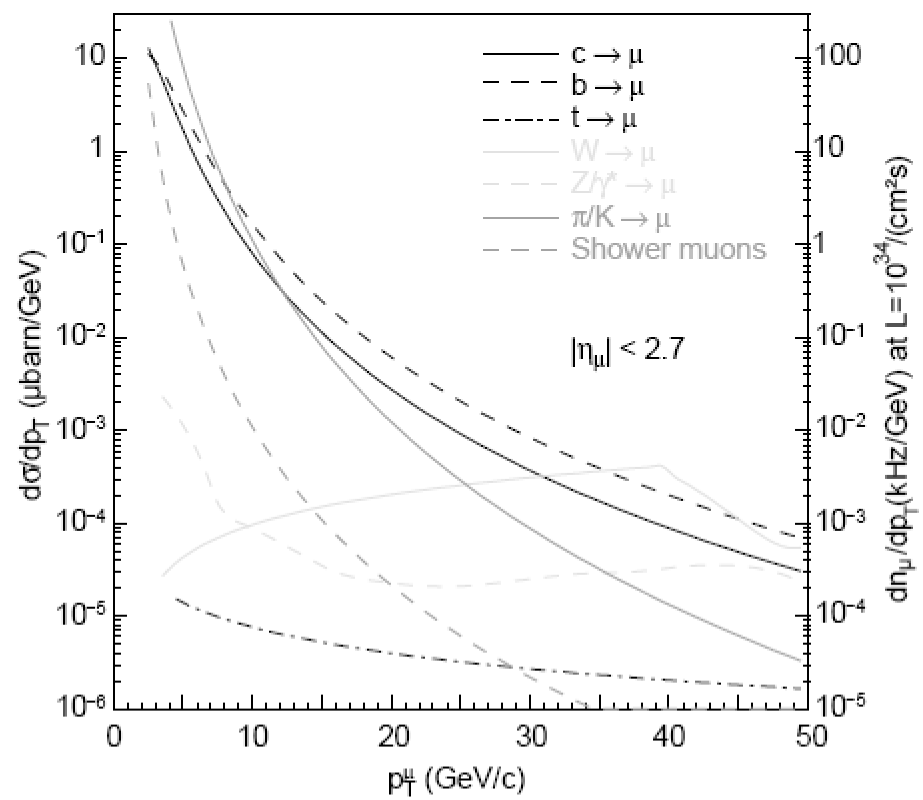

Muon identification in ATLAS

Material in front of the muon system

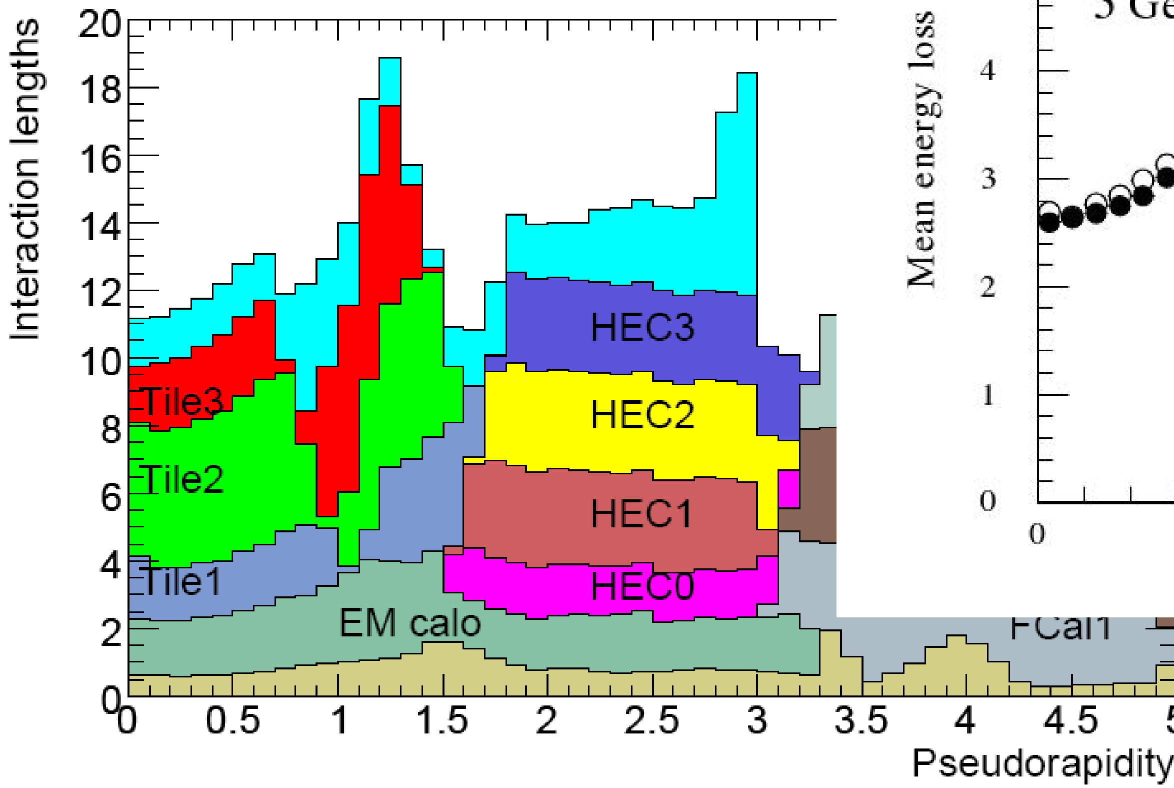

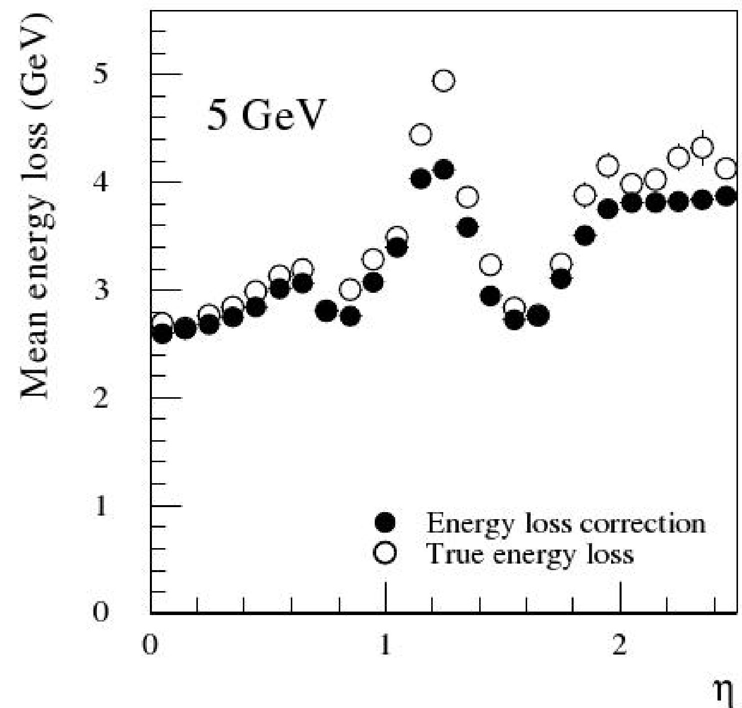

Figure 5.2: Cumulative amount of material, in units of interaction length, as a function of $|\eta|$, in front of the electromagnetic calorimeters, in the electromagnetic calorimeters themselves, in each hadronic layer, and the total amount at the end of the active calorimetry. Also shown for completeness is the total amount of material in front of the first active layer of the muon spectrometer (up to $|\eta| < 3.0$).

Muon identification efficiency

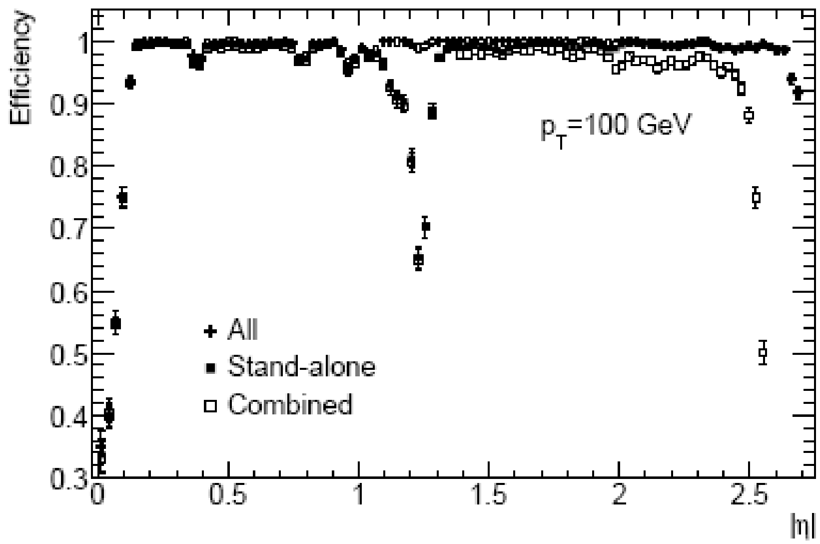

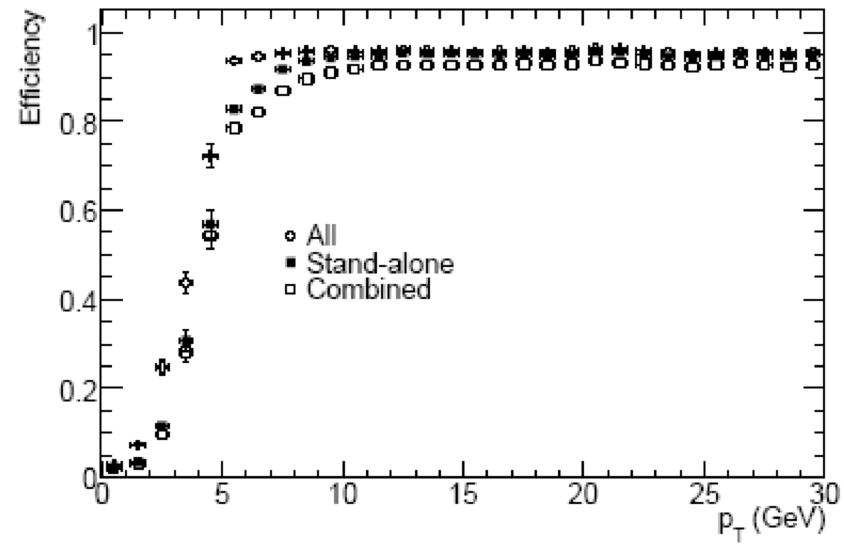

Figure 10.37: Efficiency for reconstructing muons with $p_T = 100\,\mathrm{GeV}$ as a function of $|\eta|$. The results are shown for stand-alone reconstruction, combined reconstruction and for the combination of these with the segment tags discussed in the text.

Figure 10.38: Efficiency for reconstructing muons as a function of p_T. The results are shown for stand-alone reconstruction, combined reconstruction and for the combination of these with the segment tags discussed in the text.

Muon fake probability

Sources of fakes:

-Hadrons: punch through negligible, >10 interaction legths of material in front of the muon system (remain: muons from pion and kaon decays)

-Electromagnetic showers triggered by energetic muons traversing the calorimeters and support structures lead to low-momentum electron and positron tracks, an irreducible source of fake stand-alone muons. Most of them can be rejected by a cut on their transverse momentum (pT > 5 GeV reduces the fake rate to a few percent per triggered event); can be almost entirely rejected by requiring a match of the muon-spectrometer track with an inner-detector track.

- Fake stand-alone muons from the background of thermal neutrons and low energy γ-rays in the muon spectrometer ("cavern background"). Again: pT > 5 GeV reduces this below 2% per triggered event at 10^{33} cm^{-2} s^{-1}. Can be reduced by almost an order of magnitude by requiring a match of the muon-spectrometer track with an inner-detector track.

Razpad Higgsovega delca v dva visokoenrgijska žarka gamma, H → γγ, v detektorju ATLAS

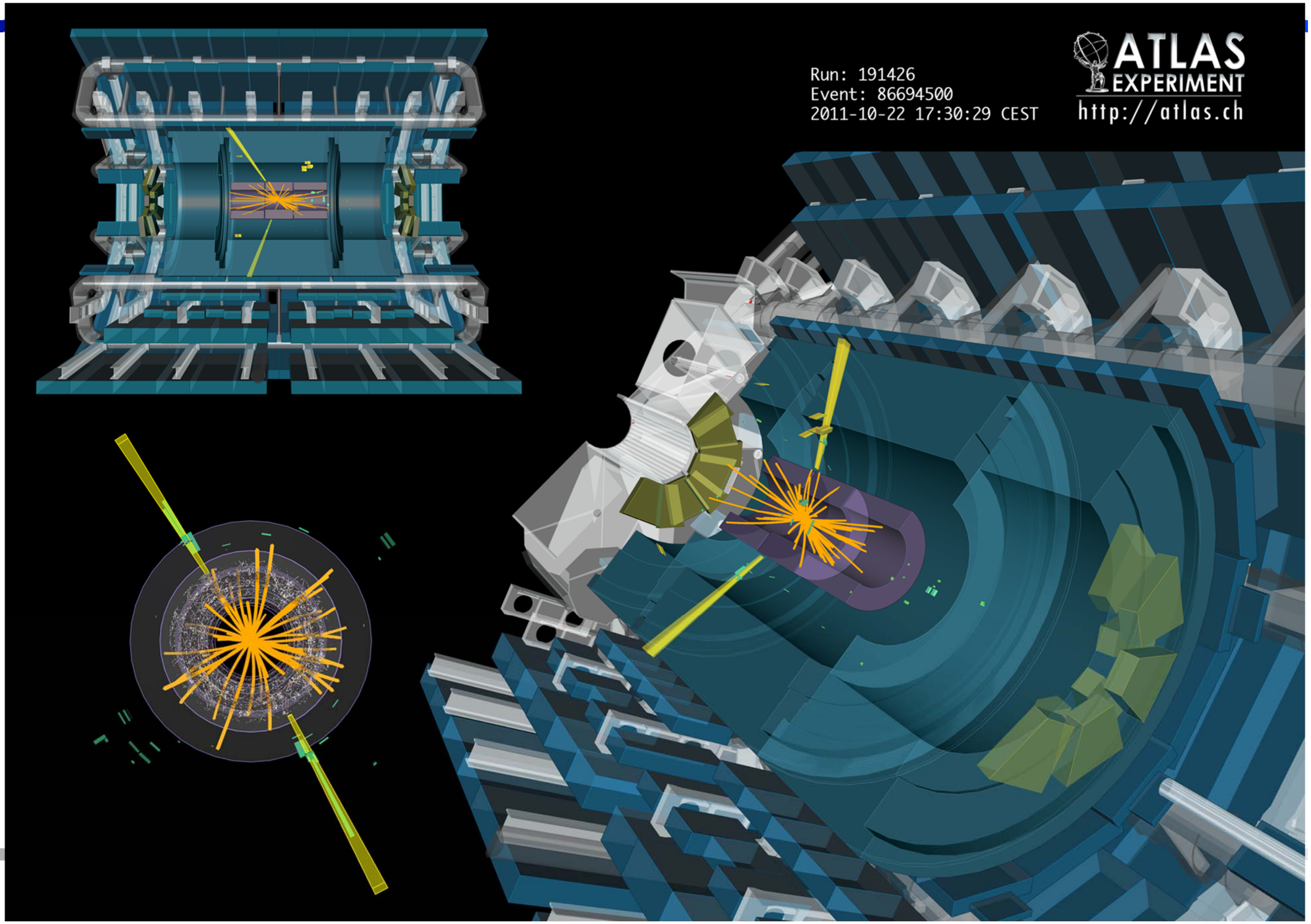

Calorimetry

Energy measurement by total absorption, combined with spatial reconstruction.

Calorimetry is a “destructive” method

Detector response α E

Calorimetry works both for

- charged ($e^\pm$ and hadrons) and
- neutral particles (n,γ)

Basic mechanism: formation of electromagnetic or hadronic showers.

Finally, the energy is converted into ionization or excitation of the matter.

Energy loss by Bremsstrahlung

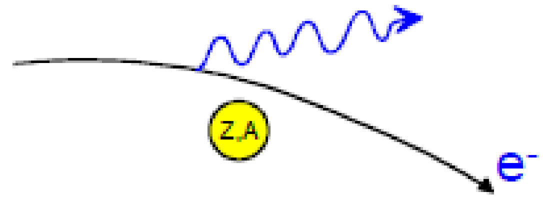

Radiation of real photons in the Coulomb field of the nuclei of the absorber

$$-\frac{dE}{dx} = 4\alpha N_A \frac{Z^2}{A} z^2 \left(\frac{1}{4\pi\varepsilon_0} \frac{e^2}{mc^2} \right)^2 E \ln \frac{183}{Z^{1/3}} \propto \frac{E}{m^2}$$

Effect plays a role only for e± and ultra-relativistic μ (>1000 GeV)

For electrons:

$$-\frac{dE}{dx} = 4\alpha N_A \frac{Z^2}{A} r_e{}^2 E \ln \frac{183}{Z^{1/3}}$$

$$-\frac{dE}{dx} = \frac{E}{X_0}$$

$$X_0 = \frac{A}{4\alpha N_A Z^2 r_e{}^2 \ln \frac{183}{Z^{1/3}}}$$

radiation length [g/cm²]

Material	Z	A	ρ [g/cm³]	X_0 [g/cm²]	λ_a [g/cm²]
Hydrogen (gas)	1	1.01	0.0899 (g/l)	63	50.8
Helium (gas)	2	4.00	0.1786 (g/l)	94	65.1
Beryllium	4	9.01	1.848	65.19	75.2
Carbon	6	12.01	2.265	43	86.3
Nitrogen (gas)	7	14.01	1.25 (g/l)	38	87.8
Oxygen (gas)	8	16.00	1.428 (g/l)	34	91.0
Aluminium	13	26.98	2.7	24	106.4
Silicon	14	28.09	2.33	22	106.0
Iron	26	55.85	7.87	13.9	131.9
Copper	29	63.55	8.96	12.9	134.9
Tungsten	74	183.85	19.3	6.8	185.0
Lead	82	207.19	11.35	6.4	194.0
Uranium	92	238.03	18.95	6.0	199.0

For Z > 6: $\lambda_a > X_0$

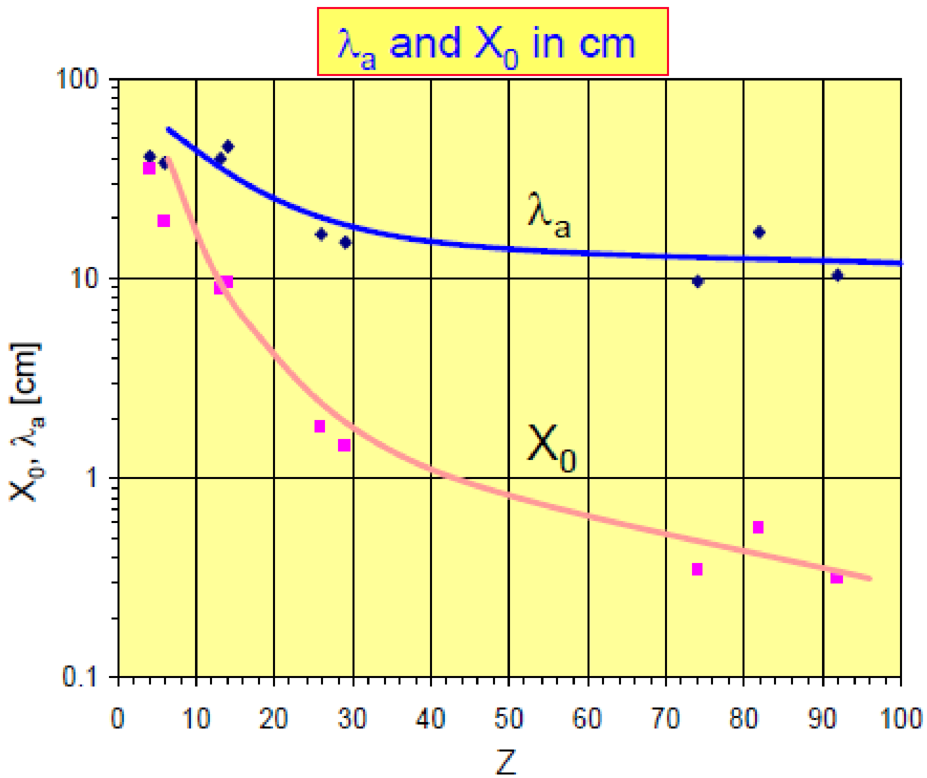

Electrons: fractional energy loss, 1/E dE/dx

Critical energy E_c

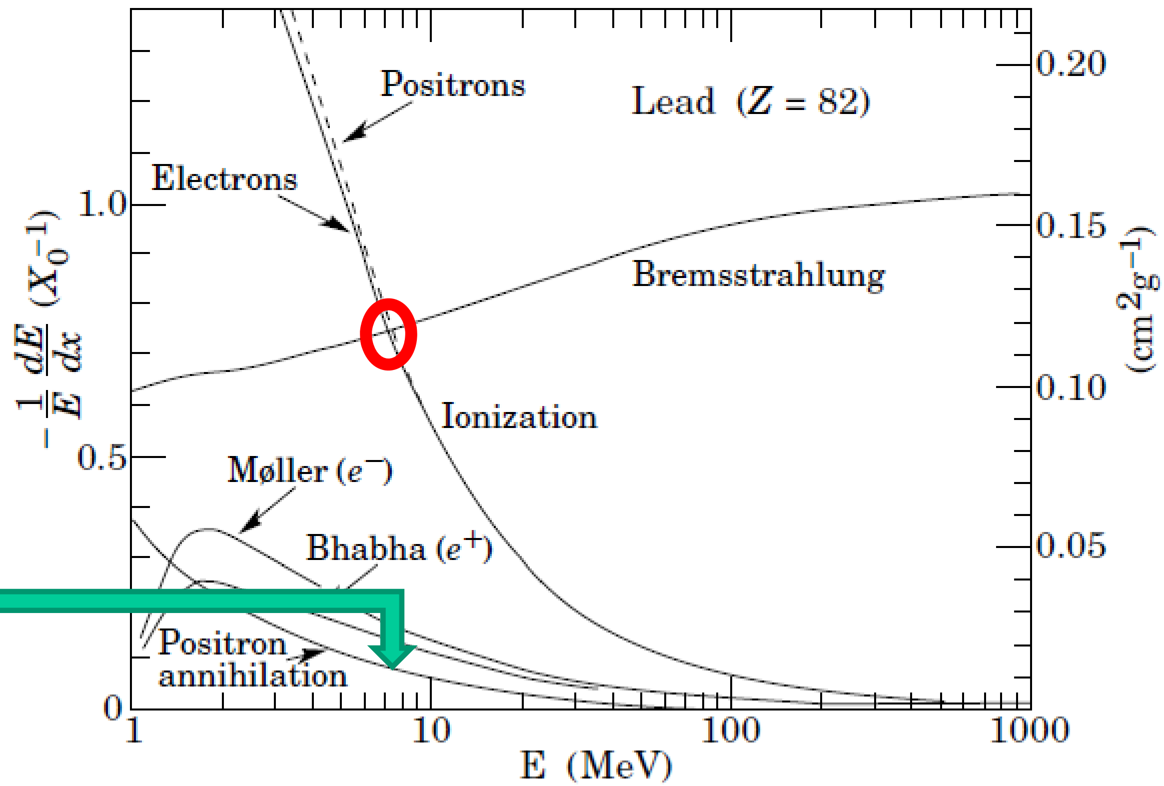

Figure 27.10: Fractional energy loss per radiation length in lead as a function of electron or positron energy. Electron (positron) scattering is considered as ionization when the energy loss per collision is below 0.255 MeV, and as Møller (Bhabha) scattering when it is above. Adapted from Fig. 3.2 from Messel and Crawford, *Electron-Photon Shower Distribution Function Tables for Lead, Copper, and Air Absorbers*, Pergamon Press, 1970. Messel and Crawford use $X_0(\mathrm{Pb}) = 5.82\ \mathrm{g/cm}^2$, but we have modified the figures to reflect the value given in the Table of Atomic and Nuclear Properties of Materials ($X_0(\mathrm{Pb}) = 6.37\ \mathrm{g/cm}^2$).

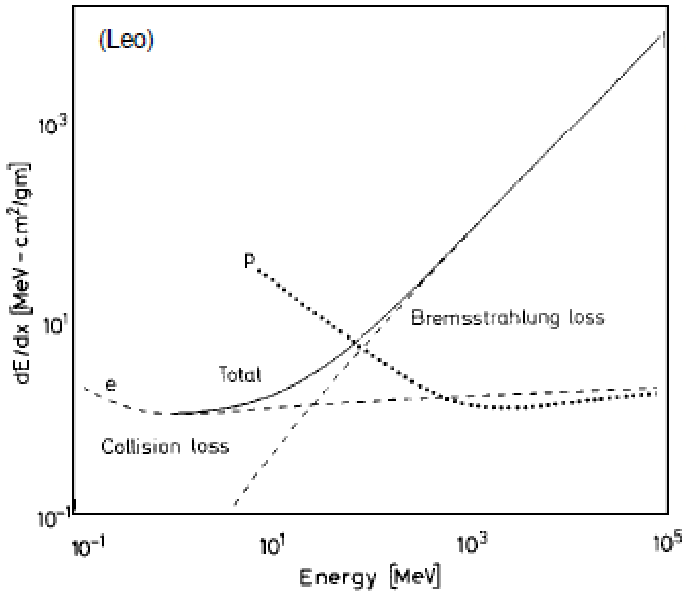

energy loss (radiative + ionization) of electrons and protons in copper

Critical energy E_c

$$\left.\frac{dE}{dx}(E_c)\right|_{Brems} = \left.\frac{dE}{dx}(E_c)\right|_{ion}$$

For electrons one finds approximately:

$$E_c^{solid+liq} = \frac{610MeV}{Z+1.24} \qquad E_c^{gas} = \frac{710MeV}{Z+1.24}$$

density effect of dE/dx(ionisation) !

$E_c(e^-)$ in Fe(Z=26) = 22.4 MeV

For muons

$$E_c \approx E_c^{elec}\left(\frac{m_\mu}{m_e}\right)^2$$

$E_c(\mu)$ in Fe(Z=26) $\approx$ 1 TeV

Interaction of photons with matter

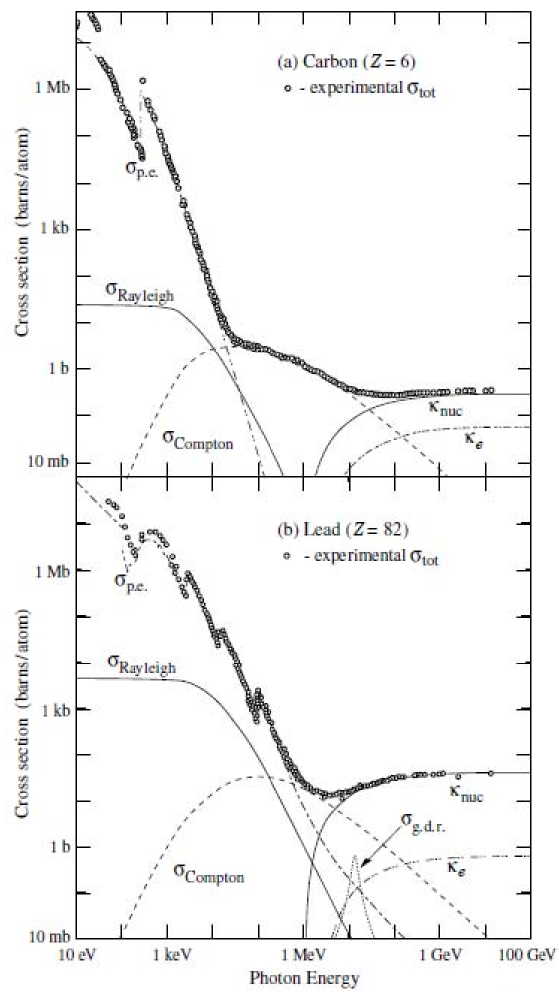

Figure 27.14: Photon total cross sections as a function of energy in carbon and lead, showing the contributions of different processes:

$\sigma_{p.e.}$ = Atomic photoelectric effect (electron ejection, photon absorption)

$\sigma_{Rayleigh}$ = Rayleigh (coherent) scattering–atom neither ionized nor excited

$\sigma_{Compton}$ = Incoherent scattering (Compton scattering off an electron)

κ_{nuc} = Pair production, nuclear field

κ_e = Pair production, electron field

$\sigma_{g.d.r.}$ = Photonuclear interactions, most notably the Giant Dipole Resonance [46]. In these interactions, the target nucleus is broken up.

Electromagnetic Cascades (showers)

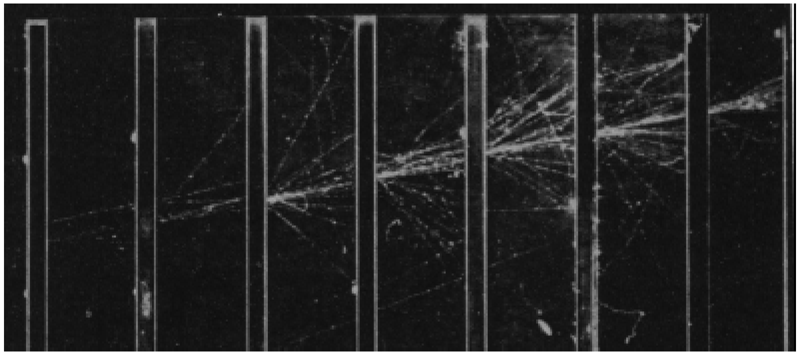

Electron shower in a cloud chamber with lead absorbers

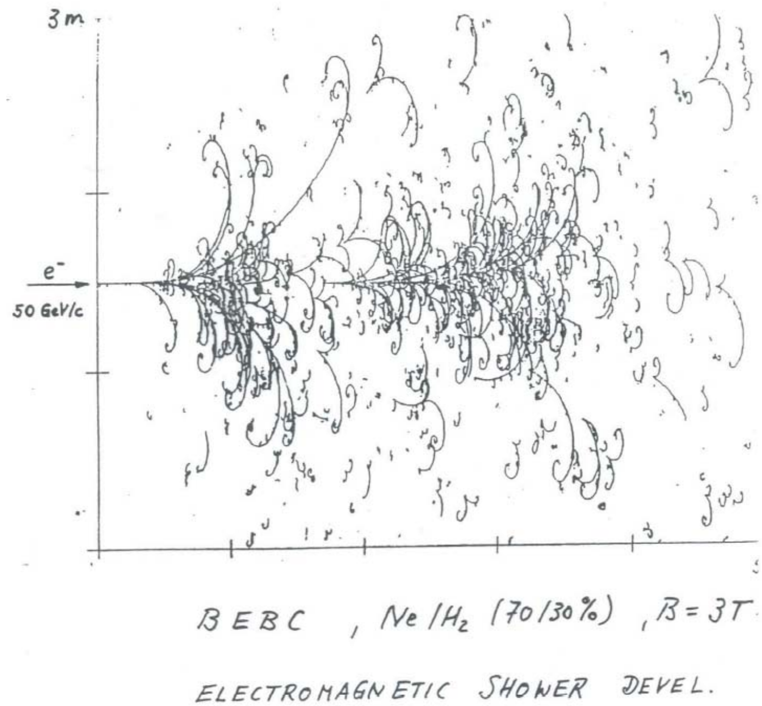

Simple qualitative model

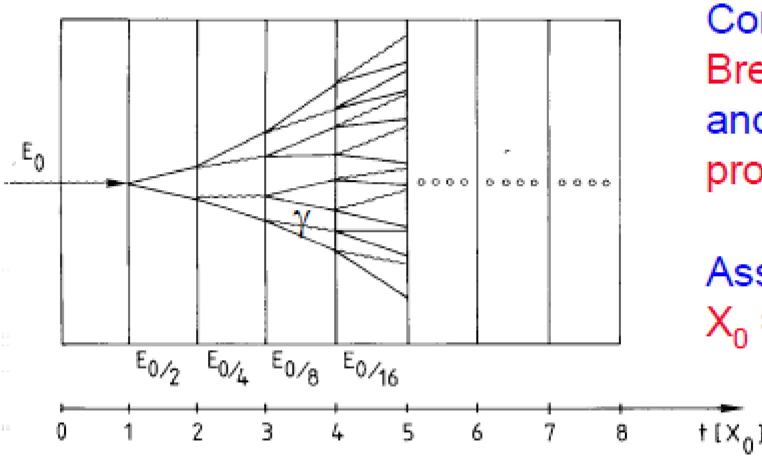

Consider only Bremsstrahlung and pair production.

Assume:

$X_0 = \lambda_{pair}$

$N(t) = 2^t \qquad E(t)/particle = E_0 \cdot 2^{-t}$

Process continues until $E(t) < E_c$

$$t_{max} = \frac{\ln E_0/E_c}{\ln 2} \qquad N^{total} = \sum_{t=0}^{t_{max}} 2^t = 2^{(t_{max}+1)} - 1 \approx 2 \cdot 2^{t_{max}} = 2\frac{E_0}{E_c}$$

After $t = t_{max}$ the dominating processes are ionization, Compton effect and photo effect → absorption.

Longitudinal shower development: $\frac{dE}{dt} \propto t^{\alpha} e^{-t}$

Shower maximum at $t_{\max} = \ln \frac{E_0}{E_c} \frac{1}{\ln 2}$

95% containment $t_{95\%} \approx t_{\max} + 0.08Z + 9.6$

Size of a calorimeter grows only logarithmically with E_0

Transverse shower development: 95% of the shower cone is located in a cylinder with radius 2 R_M

$$R_M = \frac{21\,\mathrm{MeV}}{E_c} X_0 \quad [g/cm^2]$$ Molière radius

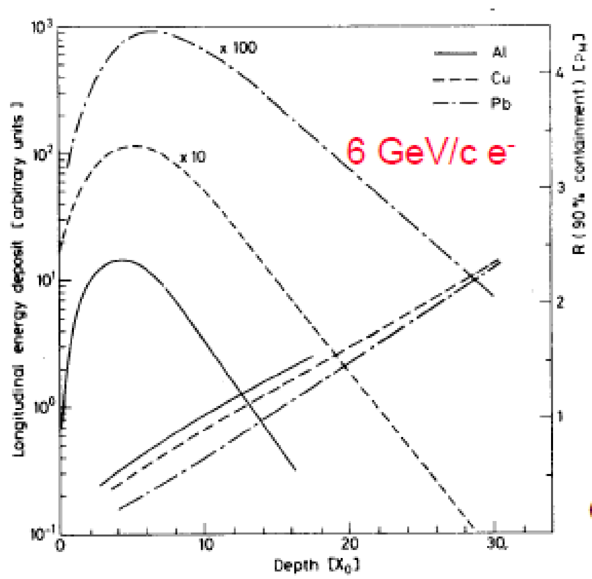

Longitudinal and transverse development scale with X_0, R_M

(C. Fabjan, T. Ludlam, CERN-EP/82-37)

Example: E_0 = 100 GeV in lead glass

E_c=11.8 MeV → $t_{max} \approx 13$, $t_{95\%} \approx 23$

$X_0 \approx 2$ cm, $R_M = 1.8 \cdot X_0 \approx 3.6$ cm

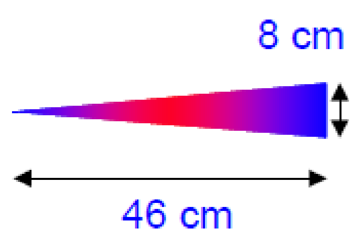

- Energy resolution of a calorimeter (intrinsic limit)

$$N^{total} \propto \frac{E_0}{E_c}$$

total number of track segments

$$\frac{\sigma(E)}{E} \propto \frac{\sigma(N)}{N} \propto \frac{1}{\sqrt{N}} \propto \frac{1}{\sqrt{E_0}}$$

holds also for hadron calorimeters

Also spatial and angular resolution scale like $1/\sqrt{E}$

Relative energy resolution of a calorimeter improves with E_0

More general:

$$\frac{\sigma(E)}{E} = \frac{a}{\sqrt{E}} \oplus b \oplus \frac{c}{E}$$

Stochastic term

Constant term

Inhomogenities
Bad cell inter-calibration
Non-linearities

Quality factor !

Noise term

Electronic noise
radioactivity
pile up

Calorimeter types

- **Homogeneous calorimeters:**
  - ⇨ Detector = absorber
  - ⇨ good energy resolution
  - ⇨ limited spatial resolution (particularly in longitudinal direction)
  - ⇨ only used for electromagnetic calorimetry

- **Sampling calorimeters:**
  - ⇨ Detectors and absorber separated → only part of the energy is sampled.
  - ⇨ limited energy resolution
  - ⇨ good spatial resolution
  - ⇨ used both for electromagnetic and hadron calorimetry

Homogeneous calorimeters

Two main types: Scintillator crystals or “glass” blocks (Cherenkov radiation).

→ photons. Readout via photomultiplier, -diode/triode

- Scintillators (crystals)

Scintillator	Density [g/cm³]	X_0 [cm]	Light Yield γ/MeV (rel. yield)	τ_1 [ns]	λ_1 [nm]	Rad. Dam. [Gy]	Comments
NaI (Tl)	3.67	2.59	4×10^4	230	415	≥10	hydroscopic, fragile
CsI (Tl)	4.51	1.86	5×10^4 (0.49)	1005	565	≥10	Slightly hygroscopic
CSI pure	4.51	1.86	4×10^4 (0.04)	10 36	310 310	10^3	Slightly hygroscopic
BaF_2	4.87	2.03	10^4 (0.13)	0.6 620	220 310	10^5	
BGO	7.13	1.13	8×10^3	300	480	10	
$PbW0_4$	8.28	0.89	≈100	10 10	≈440 ≈530	10^4	light yield =f(T)

Relative light yield: rel. to NaI(Tl) readout with PM (bialkali PC)

- Cherenkov radiators

Material	Density [g/cm³]	X_0 [cm]	n	Light yield [p.e./GeV] (rel. p.e.)	λ_{cut} [nm]	Rad. Dam. [Gy]	Comments
SF-5 Lead glass	4.08	2.54	1.67	600 (1.5×10^{-4})	350	10^2	
SF-6 Lead glass	5.20	1.69	1.81	900 (2.3×10^{-4})	350	10^2	
PbF_2	7.66	0.95	1.82	2000 (5×10^{-4})		10^3	Not available in quantity

Relative light yield: rel. to NaI(Tl) readout with PM (bialkali PC)

Sampling calorimeters

Absorber + detector separated $\rightarrow$ additional sampling fluctuations

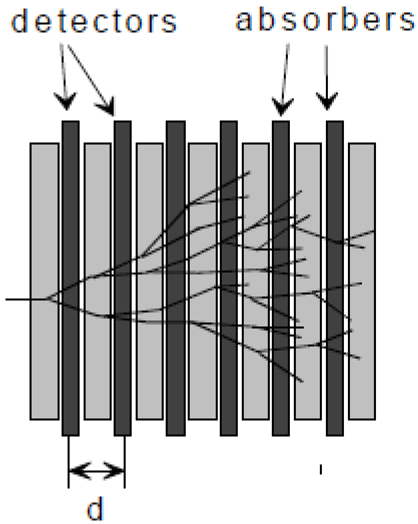

$$N = \frac{T_{\det}}{d}$$ Detectable track segments

$$= F(\xi)\frac{E}{E_c} X_0 \frac{1}{d}$$

$$\frac{\sigma(E)}{E} \propto \frac{\sqrt{N}}{N} \propto \sqrt{\frac{1}{E}} \cdot \sqrt{\frac{d}{X_0}}$$

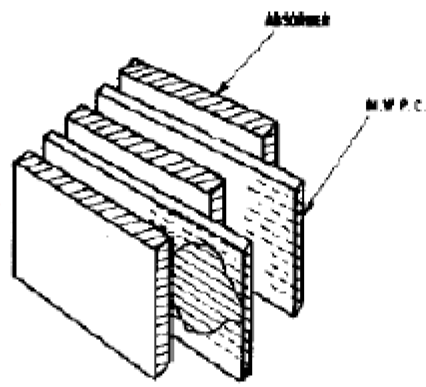

- MWPC, streamer tubes
- warm liquids
  - TMP = tetramethylpentane,
  - TMS = tetramethylsilane
- cryogenic noble gases:
  - mainly LAr (Lxe, LKr)
- scintillators, scintillation fibres, silicon detectors

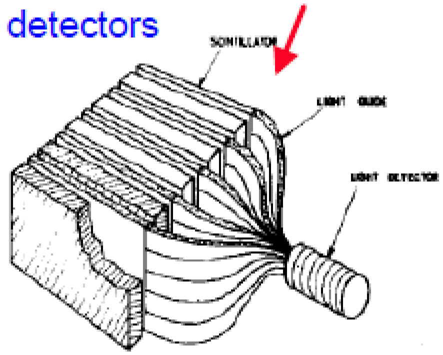

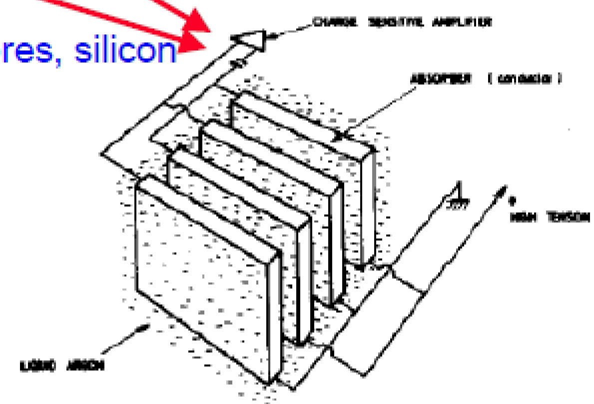

◆ ATLAS electromagnetic Calorimeter

Accordion geometry absorbers immersed in Liquid Argon

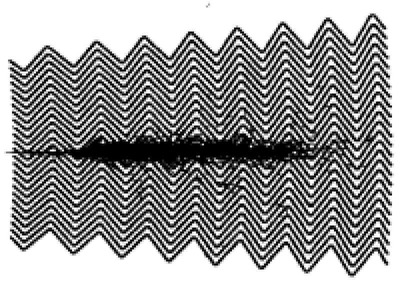

(RD3 / ATLAS)

Liquid Argon (90K)
+ lead-steal absorbers (1-2 mm)
+ multilayer copper-polyimide
  readout boards
→ Ionization chamber.
1 GeV E-deposit → 5 x10^6 e$^-$

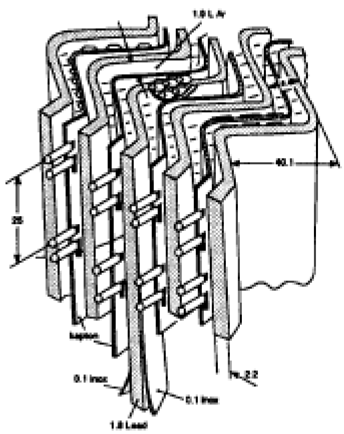

- Accordion geometry minimizes dead zones.
- Liquid Ar is intrinsically radiation hard.
- Readout board allows fine segmentation (azimuth, pseudo-rapidity and longitudinal) acc. to physics needs

Test beam results, e$^-$ 300 GeV (ATLAS TDR)

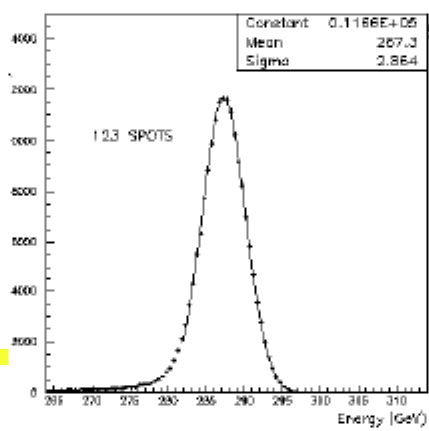

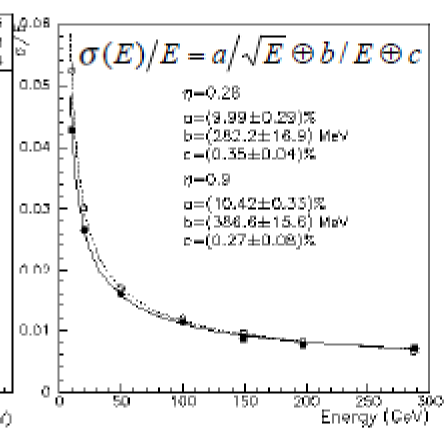

Spatial and angular uniformity ≈0.5%

Spatial resolution ≈ 5mm / E$^{1/2}$

Nuclear Interactions

The interaction of energetic hadrons (charged or neutral) is determined by inelastic nuclear processes.

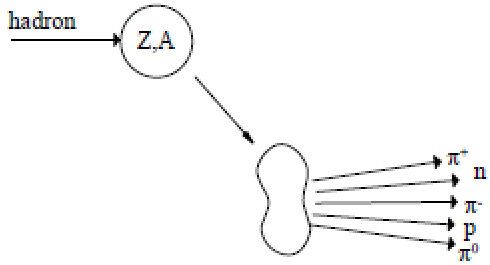

multiplicity $\propto \ln(E)$

$p_t \approx 0.35$ GeV/c

Excitation and finally breakup up nucleus → nucleus fragments + production of secondary particles.

For high energies (>1 GeV) the cross-sections depend only little on the energy and on the type of the incident particle (p, π, K…).

$$\sigma_{inel} \approx \sigma_0 A^{0.7} \quad \sigma_0 \approx 35\ mb$$

In analogy to X_0 a hadronic absorption length can be defined

$$\lambda_a = \frac{A}{N_A \sigma_{inel}} \propto A^{\frac{1}{4}} \quad \text{because } \sigma_{inel} \approx \sigma_0 A^{0.7}$$

similarly a hadronic interaction length

$$\lambda_I = \frac{A}{N_A \sigma_{total}} \propto A^{\frac{1}{3}} \qquad \lambda_I < \lambda_a$$

Material	Z	A	ρ [g/cm³]	X_0 [g/cm²]	λ_a [g/cm²]
Hydrogen (gas)	1	1.01	0.0899 (g/l)	63	50.8
Helium (gas)	2	4.00	0.1786 (g/l)	94	65.1
Beryllium	4	9.01	1.848	65.19	75.2
Carbon	6	12.01	2.265	43	86.3
Nitrogen (gas)	7	14.01	1.25 (g/l)	38	87.8
Oxygen (gas)	8	16.00	1.428 (g/l)	34	91.0
Aluminium	13	26.98	2.7	24	106.4
Silicon	14	28.09	2.33	22	106.0
Iron	26	55.85	7.87	13.9	131.9
Copper	29	63.55	8.96	12.9	134.9
Tungsten	74	183.85	19.3	6.8	185.0
Lead	82	207.19	11.35	6.4	194.0
Uranium	92	238.03	18.95	6.0	199.0

For Z > 6: $\lambda_a > X_0$

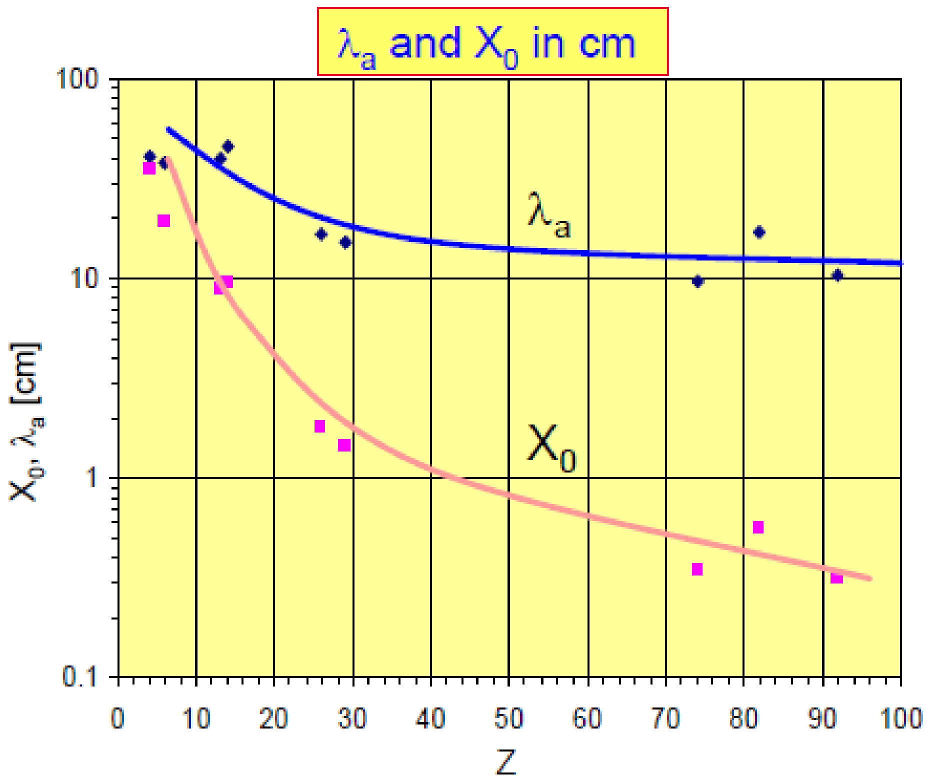

Hadronic casacdes

Various processes involved. Much more complex than electromagnetic cascades.

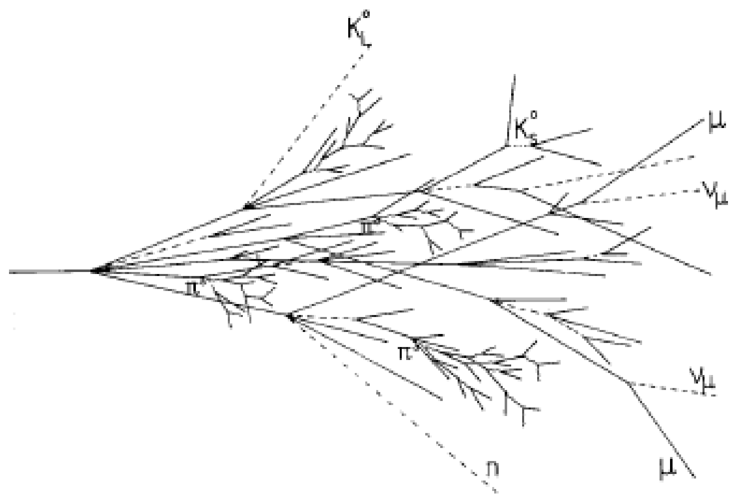

(Grupen)

Hadronic + electromagnetic component

↓

charged pions, protons, kaons ….

Breaking up of nuclei

(binding energy),

neutrons, neutrinos, soft γ's

muons …. → invisible energy

↓

neutral pions → 2γ →

electromagnetic cascade

$$n(\pi^0) \approx \ln E(GeV) - 4.6$$

example 100 GeV: $n(\pi^0) \approx 18$

Large energy fluctuations → limited energy resolution

Longitudinal shower development

$$t_{max}(\lambda_I) \approx 0.2 \ln E[GeV] + 0.7$$

$$t_{95\%} \approx a \ln E + b$$

For Iron: a = 9.4, b=39
E =100 GeV
→ $t_{95\%} \approx$ 80 cm

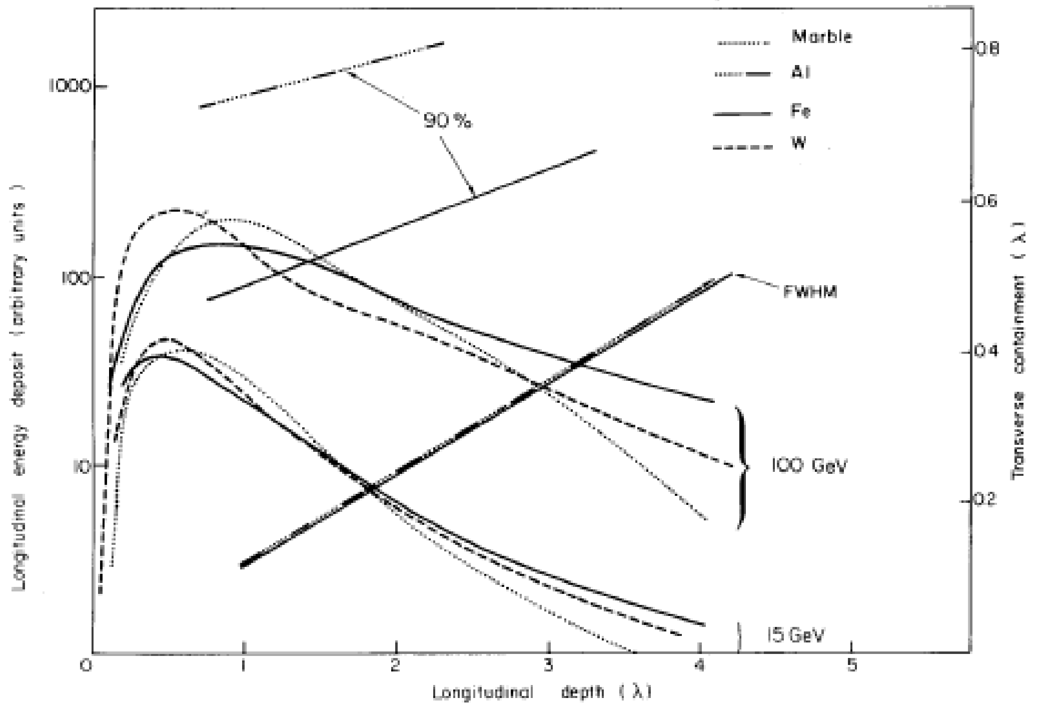

(C. Fabjan, T. Ludlam, CERN-EP/82-37)

Hadronic showers are much longer and broader than electromagnetic ones!

Laterally shower consists of core + halo.
95% containment in a cylinder of radius λ_I.

Iron: λ_I=16.7 cm

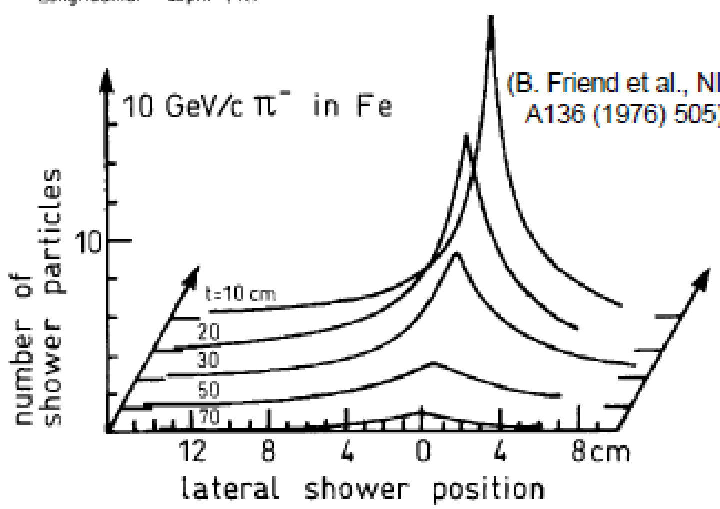

(B. Friend et al., NIM A136 (1976) 505)

◆ CMS Hadron calorimter

Cu absorber + scintillators

↓

2 x 18 wedges (barrel)
+ 2 x 18 wedges (endcap) ≈ 1500 T absorber

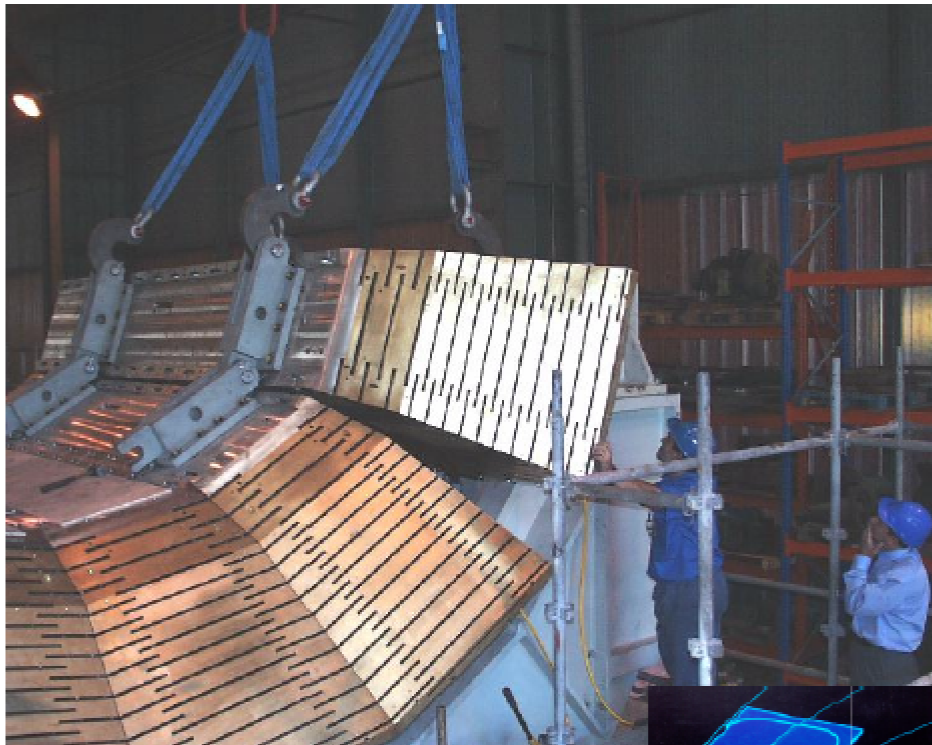

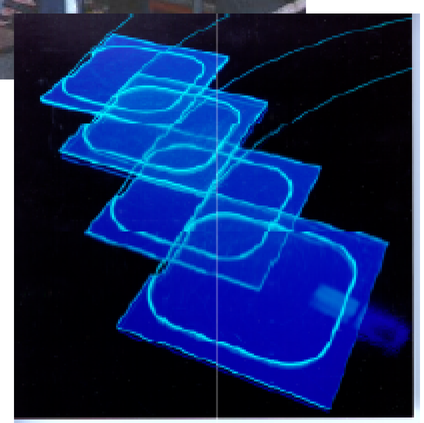

Scintillators fill slots and are read out via fibres by HPDs

Test beam resolution for single hadrons $$\frac{\sigma_E}{E} = \frac{65\%}{\sqrt{E}} \oplus 5\%$$

4 scintillating tiles of the CMS Hadron calorimeter

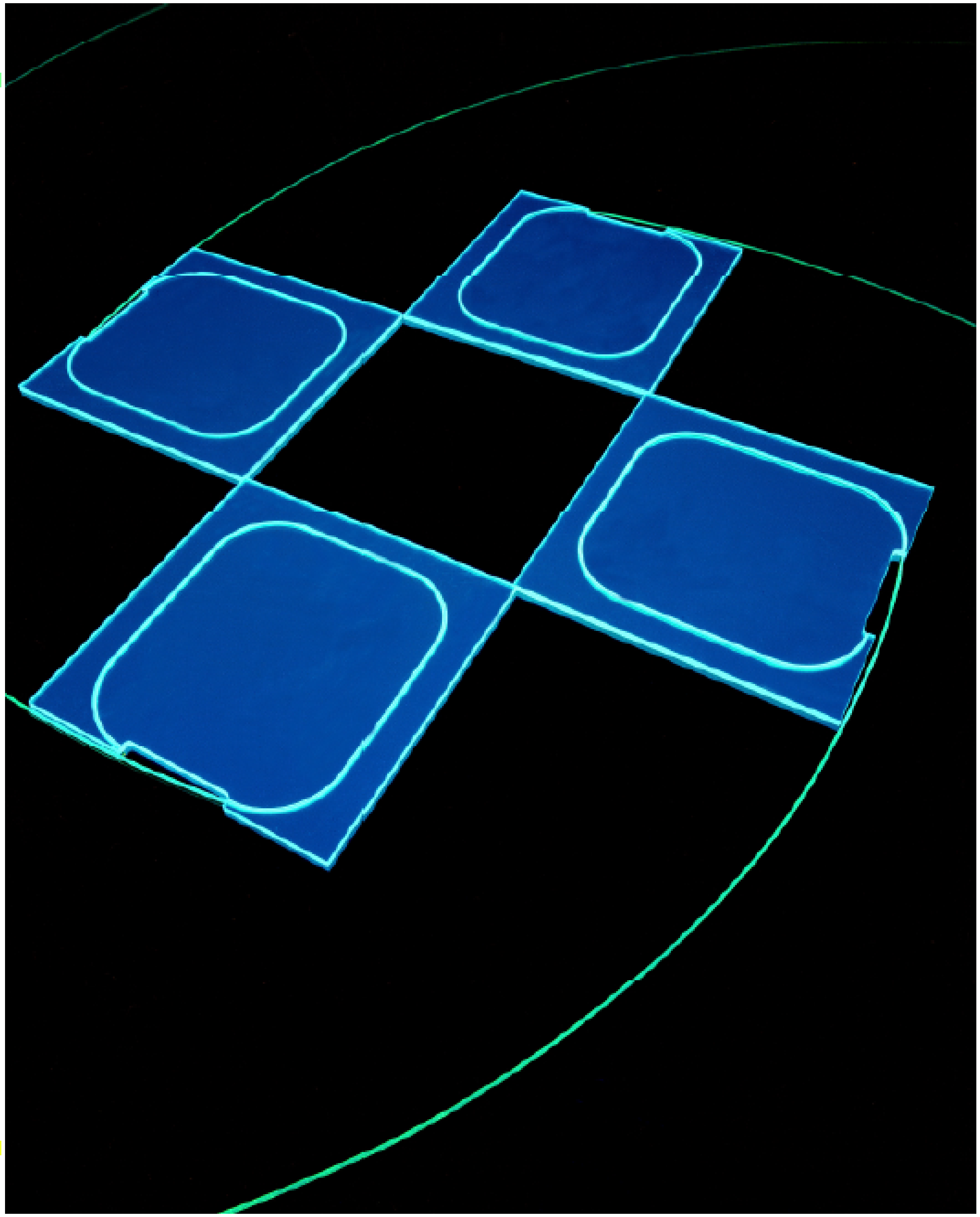

Detektor ATLAS med gradnjo

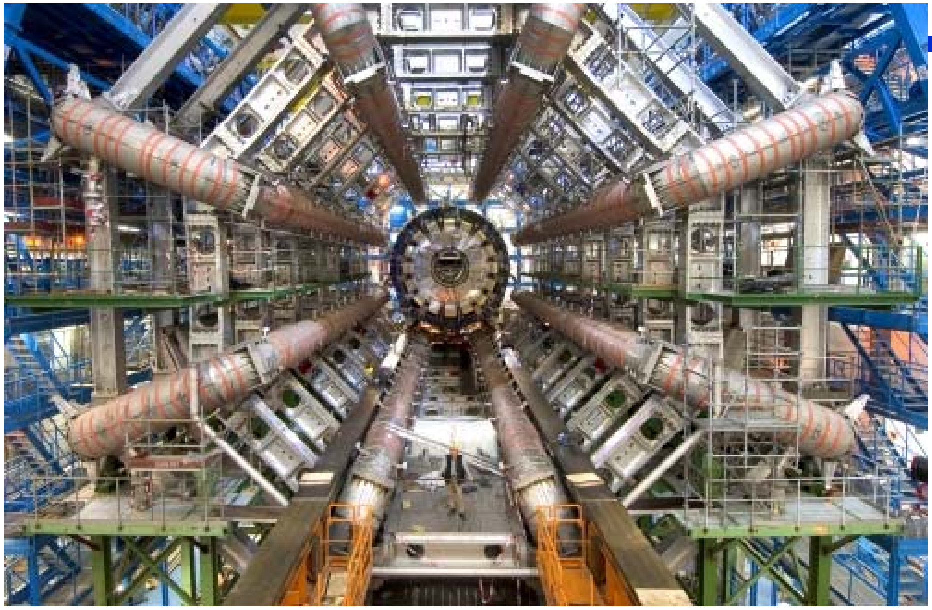

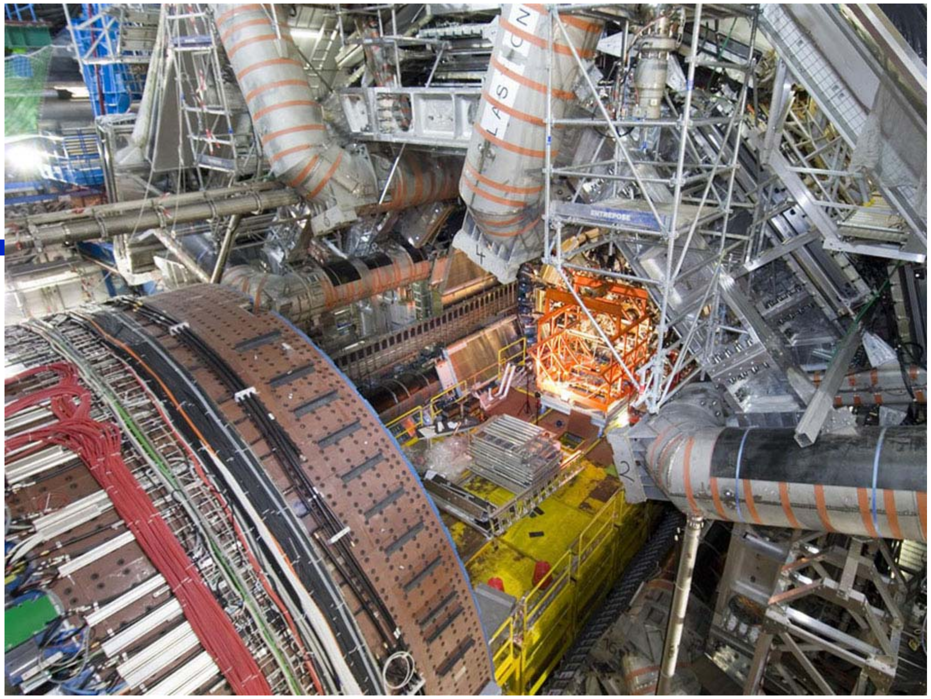

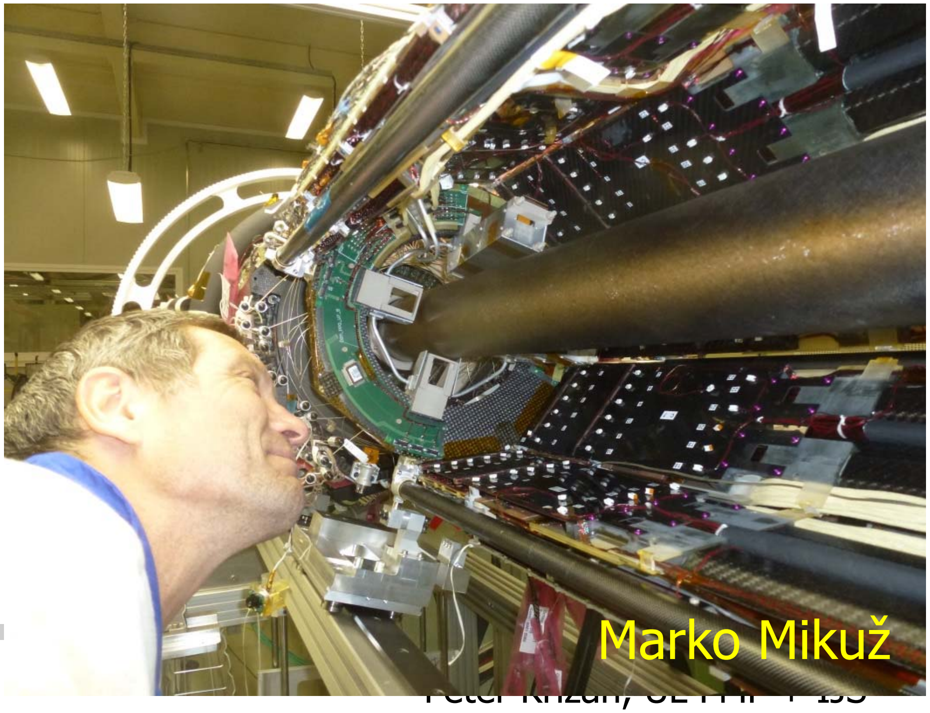

Viden delež slovenske raziskovalne skupine (IJS in FMF UL)

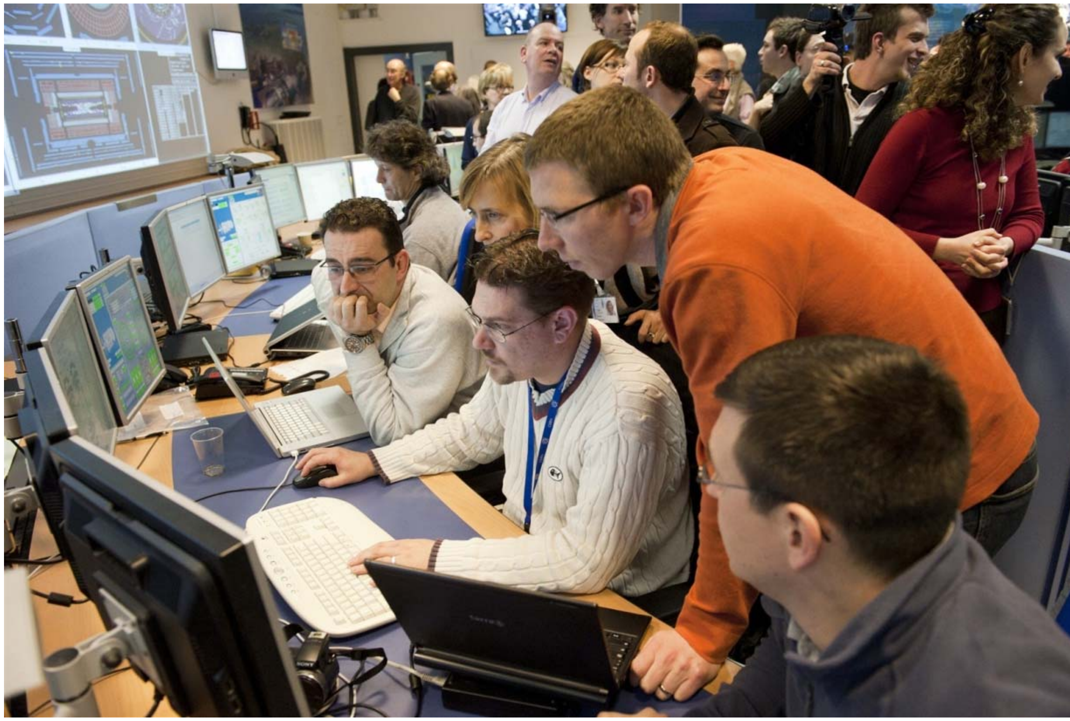

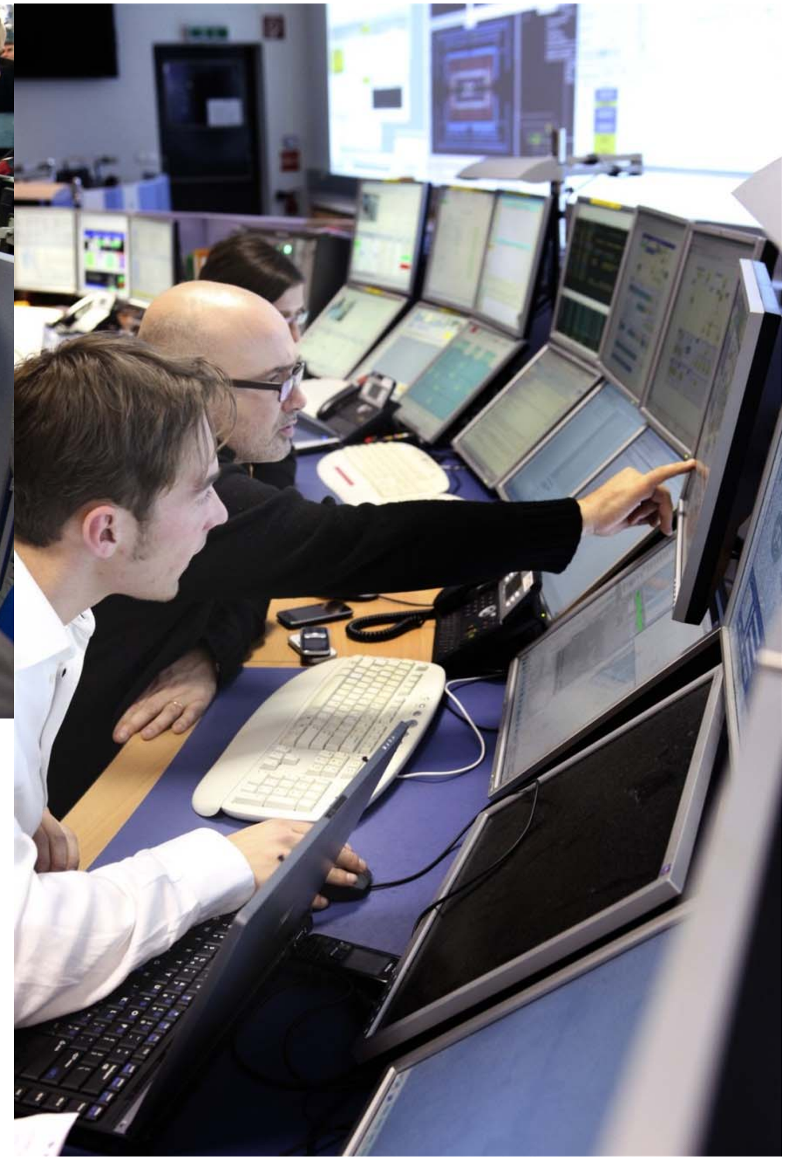

Kontrolna soba med meritvami...

Iskanje Higgsove delca z detektorjema ATLAS in CMS ob LHC

- Trkalnik in oba velika detektorja, ATLAS in CMS odlično delujejo od konca leta 2009

- Julij 2012: ATLAS in CMS objavita odkritje Higgsovega bozona – pravzaprav delca, za katerega zaenkrat vse kaže, da ima take lastnosti, kot jih pričakujemo od Higgsovega delca (‘Higgs-like particle’).

- Na dokončno potrditev je bilo treba počakati do 2013, ko so nabrali dovolj velik vzorec podatkov, da so lahko opravili dodatne meritve.

Rezultat meritve: iskanje razpada Higgsovega bozona v dva žarka gamma, H → $\gamma\gamma$

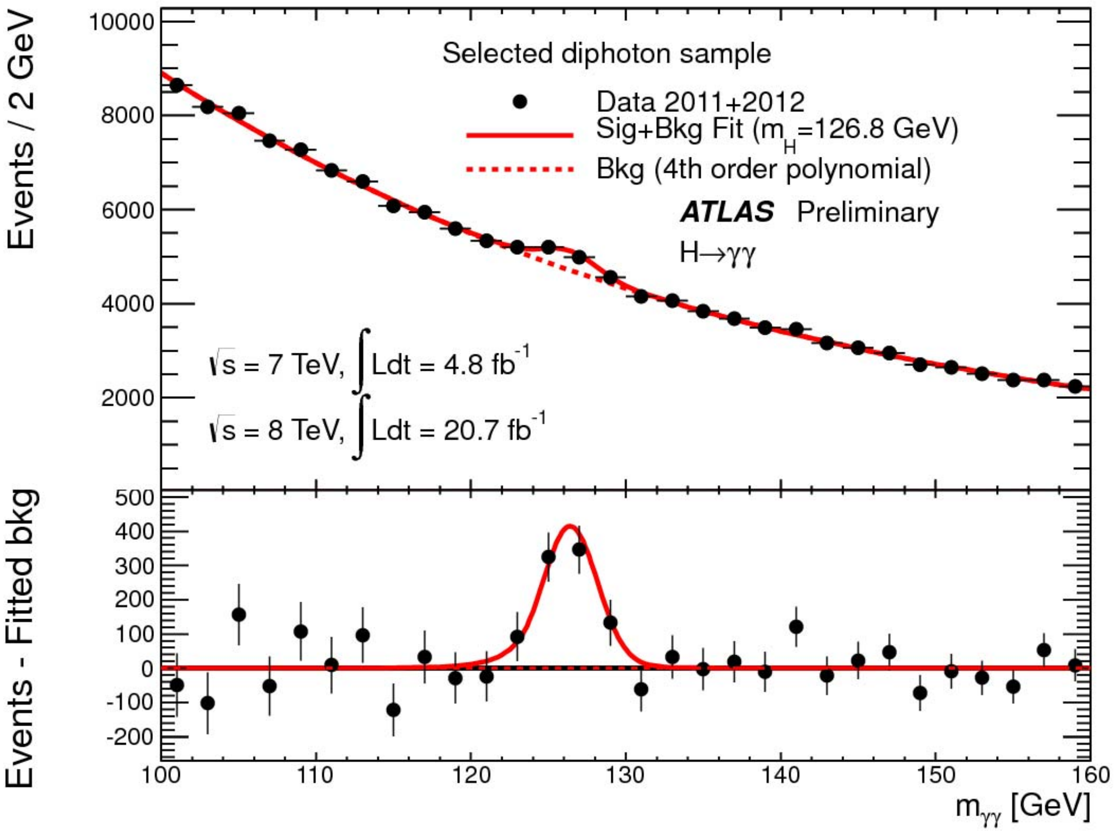

Masa vsake zabeležene kombinacije dveh visokoenergijskih žarkov gama:

– veliko večino predstavljajo naključne kombinacije
- vrh pri energiji 126 GeV ustreza razpadom H → $\gamma\gamma$

Izmerjena porazdelitev minus ozadje → signal!

Rezultat meritve: iskanje razpada Higgsovega bozona v dva žarka gamma, H → $\gamma\gamma$

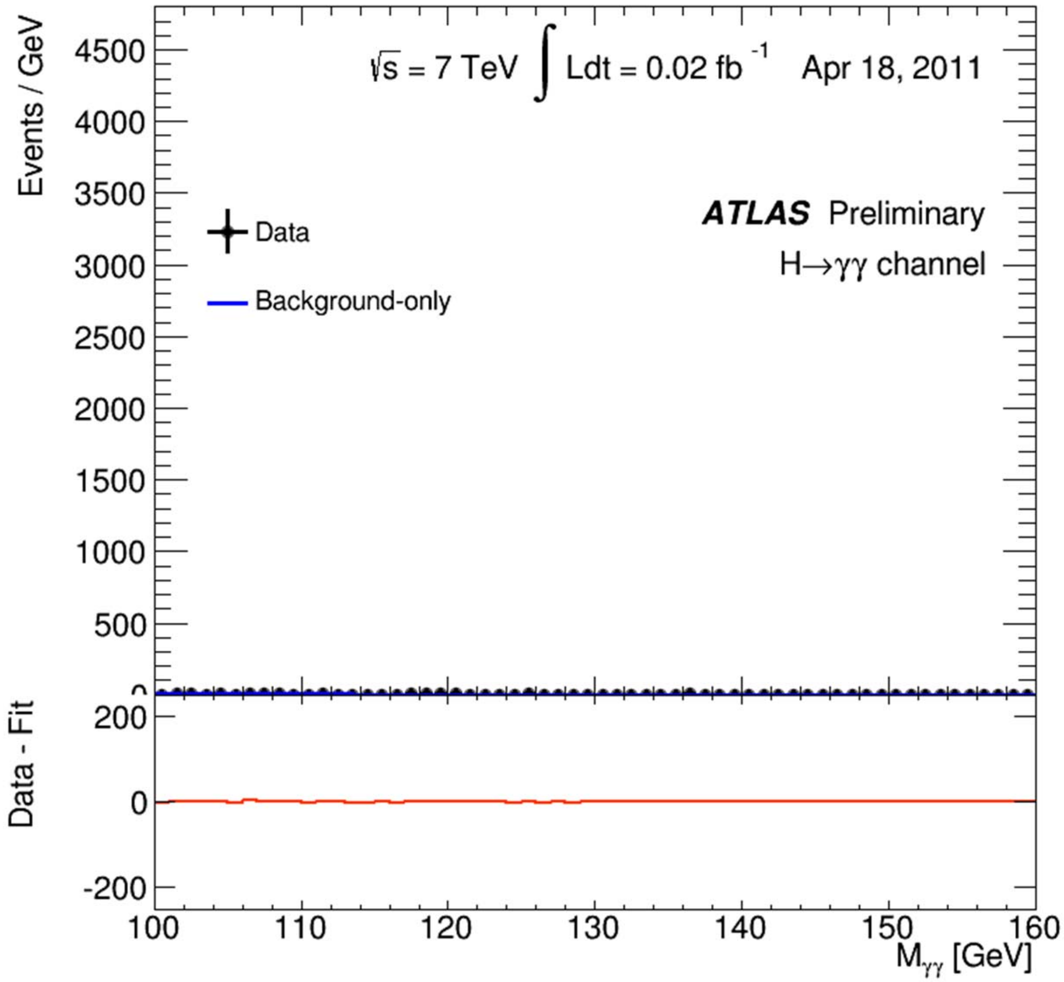

Odkritje Higgsovega delca

Na dokončno potrditev je bilo treba počakati do 2013, ko so nabrali dovolj velik vzorec podatkov, da so lahko opravili dodatne meritve.

- Primerjava števila razpadov Higgsovega bozona v različnih razpadnih kanalih
- Kotne porazdelitve delcev v končnem stanju – določanje lastnosti tega delca (spin – vrtilna količina).

→ Novi delec ima take lastnosti, kot jih predvideva Standardni model

Nobelova nagrada 2013!

Francois Englert in Peter W. Higgs

Rezultat meritve: iskanje razpada Higgsovega bozona v štiri leptone, H → $\mu^+ \mu^- \mu^+ \mu^-$

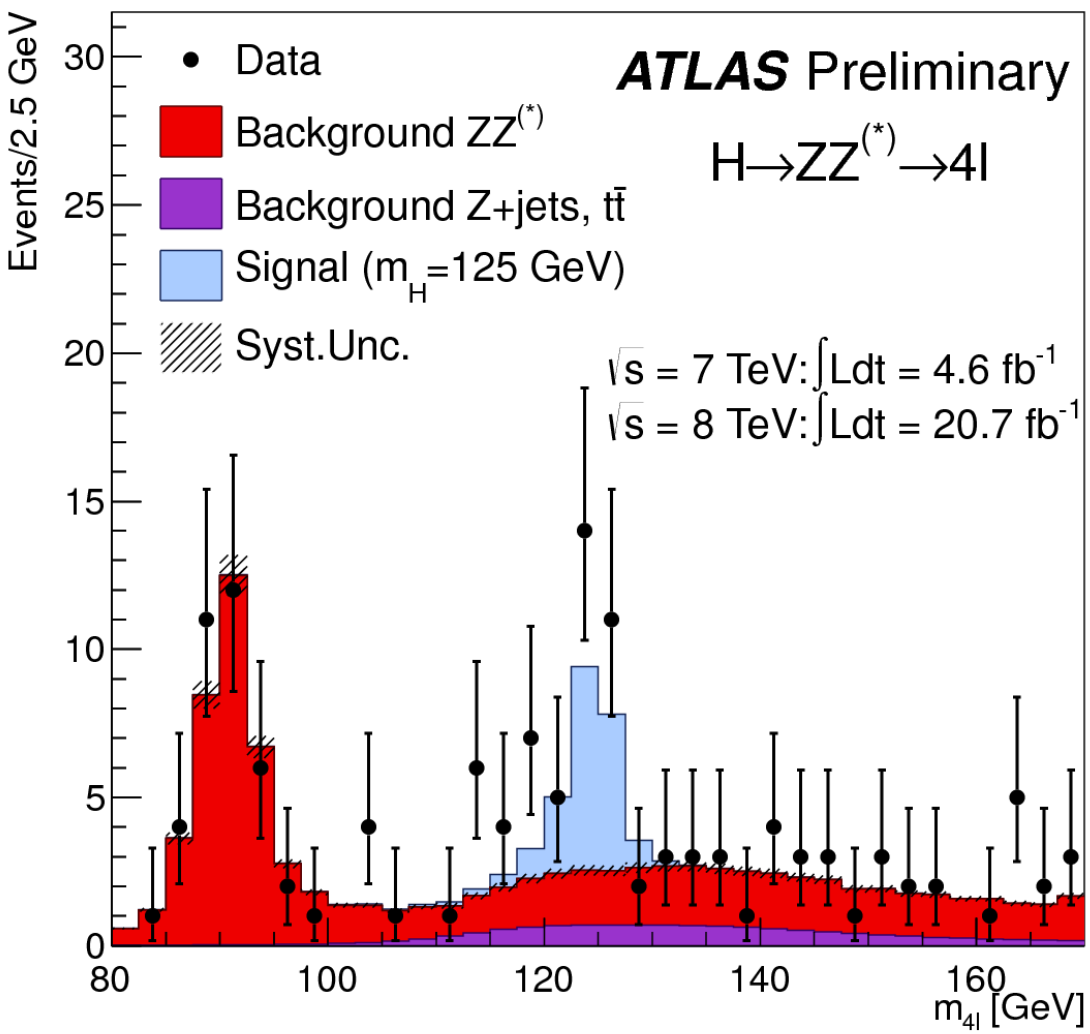

Masa vsake zabeležene kombinacije štirih mionov – večinoma kombinacije drugih procesov - ozadja (rdeče in vijolično).

Modro: signal, kot bi ga pričakovali za Higgsov delec

Heavy ion collisions: ALICE

Goals:

- Search for a new state of matter: quark-gluon plasma

Challenge: several thousand particles produced in a collision of two Pb nuclei.

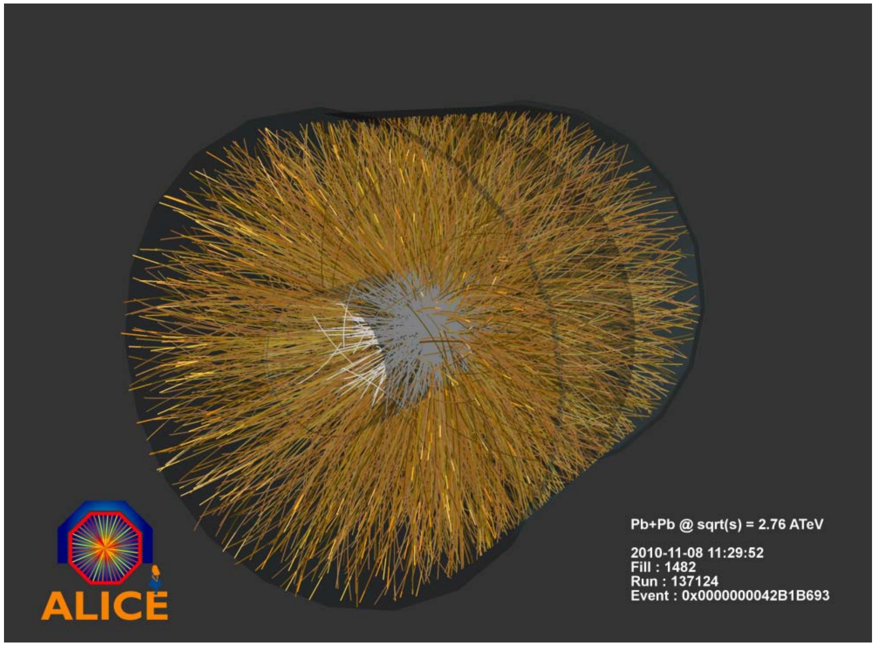

Tracking in ALICE: a time-projection chamber (TPC)

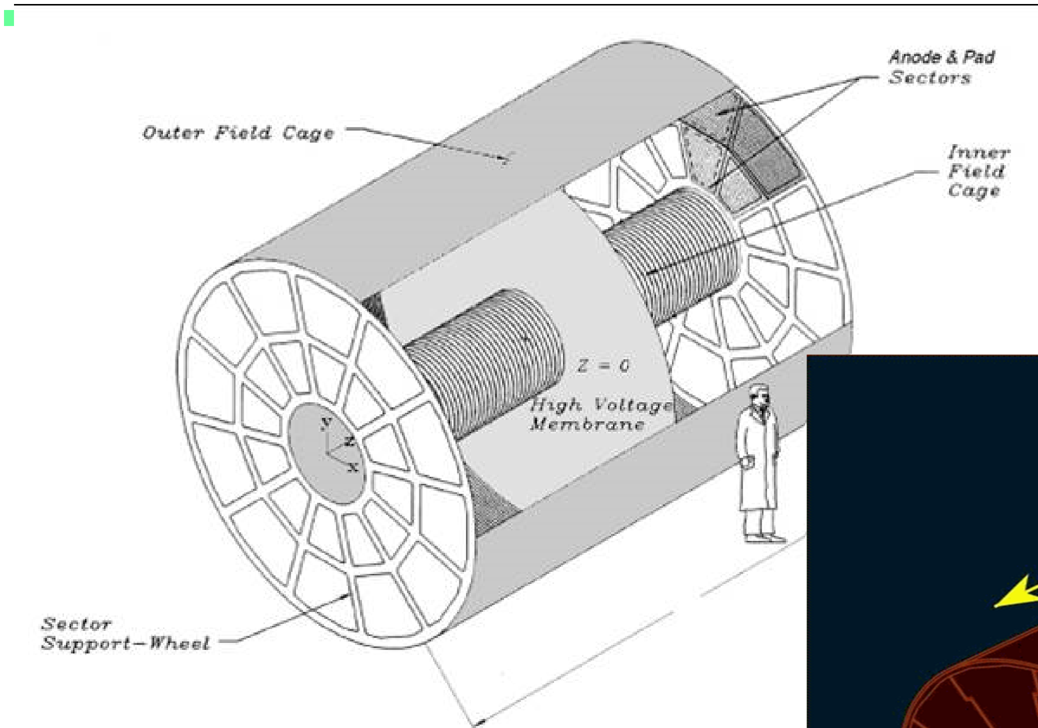

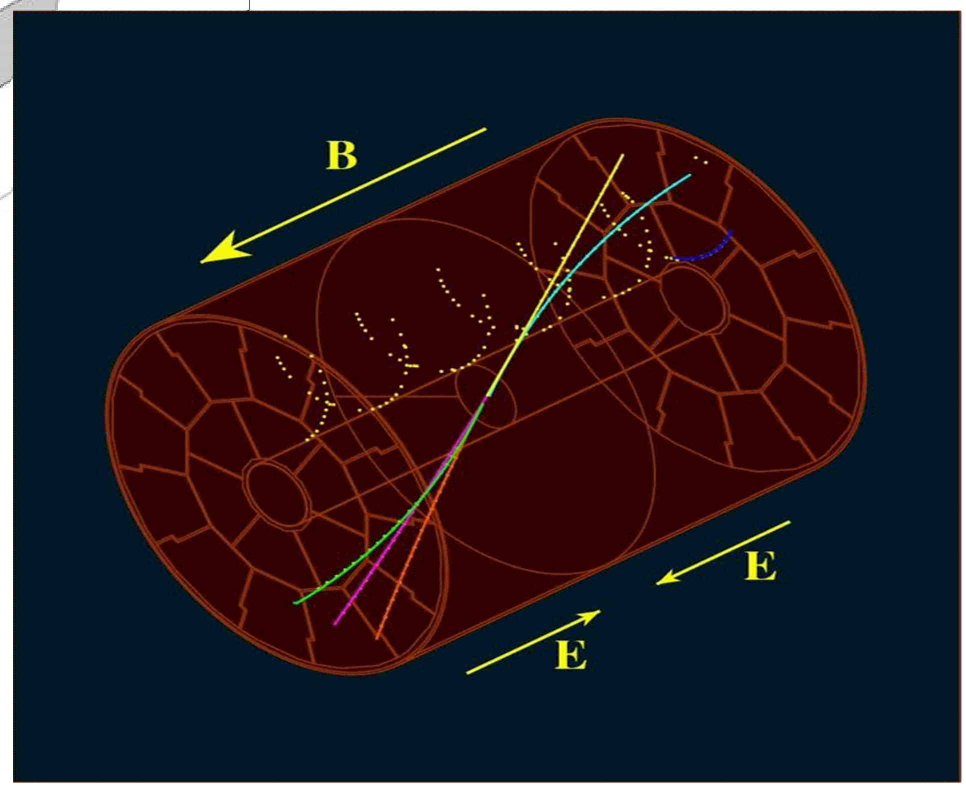

Identification with the dE/dx measurement

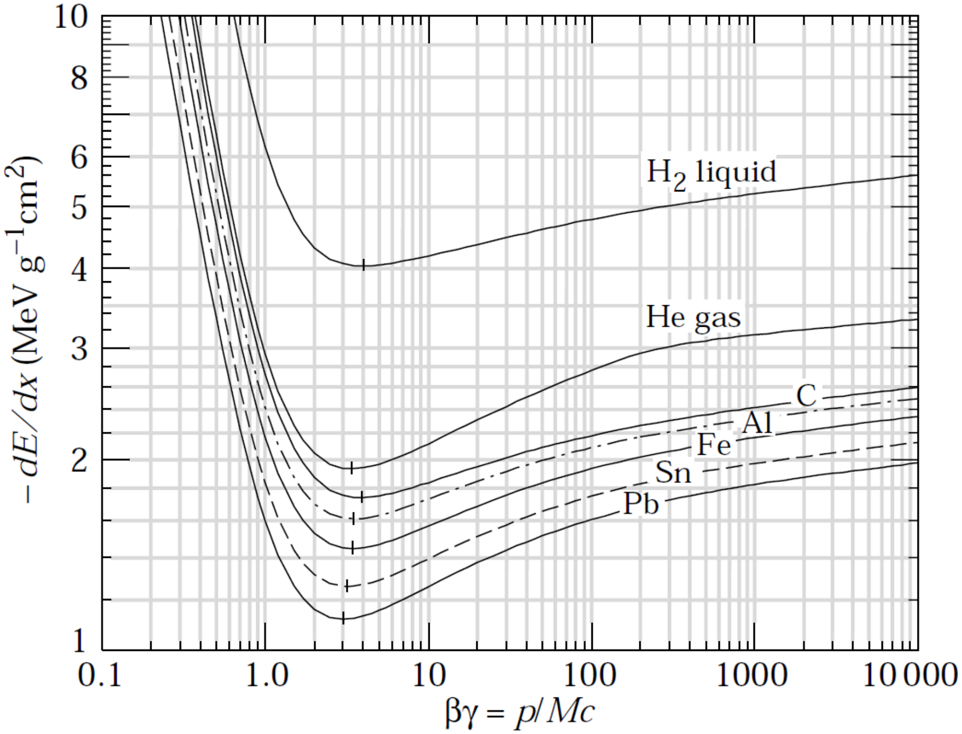

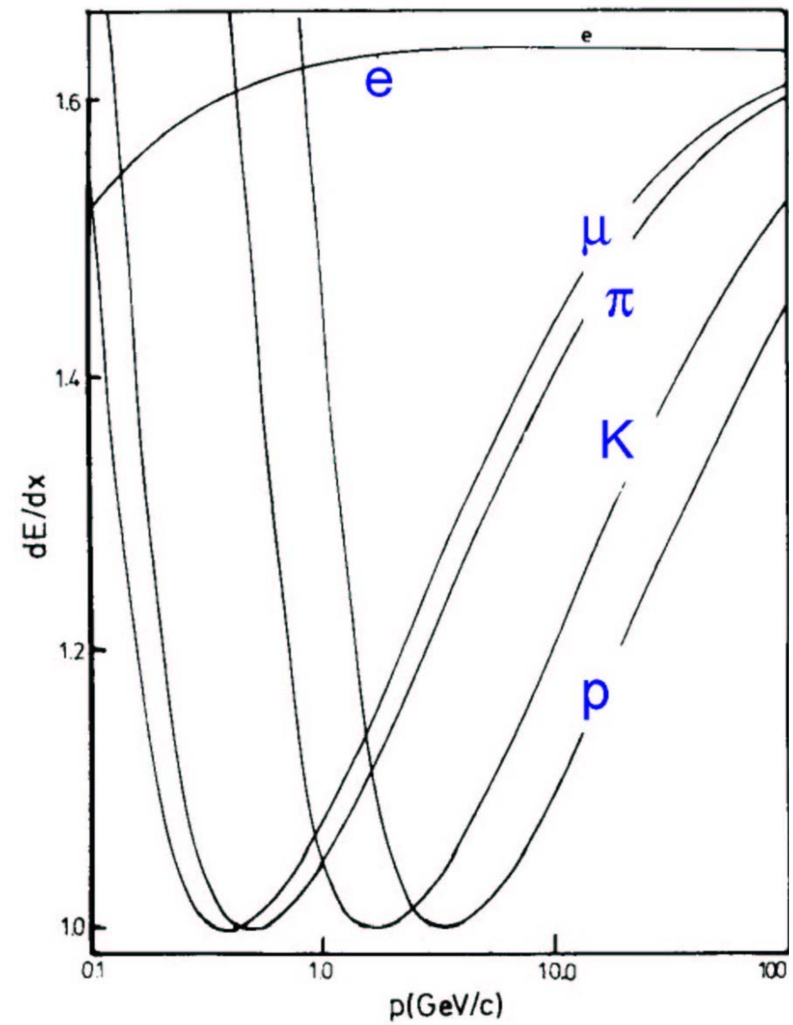

dE/dx is a function of velocity β

For particles with different mass the Bethe-Bloch curve gets displaced if plotted as a function of p

For good separation: resolution should be ~5%

dE/dx in ALICE

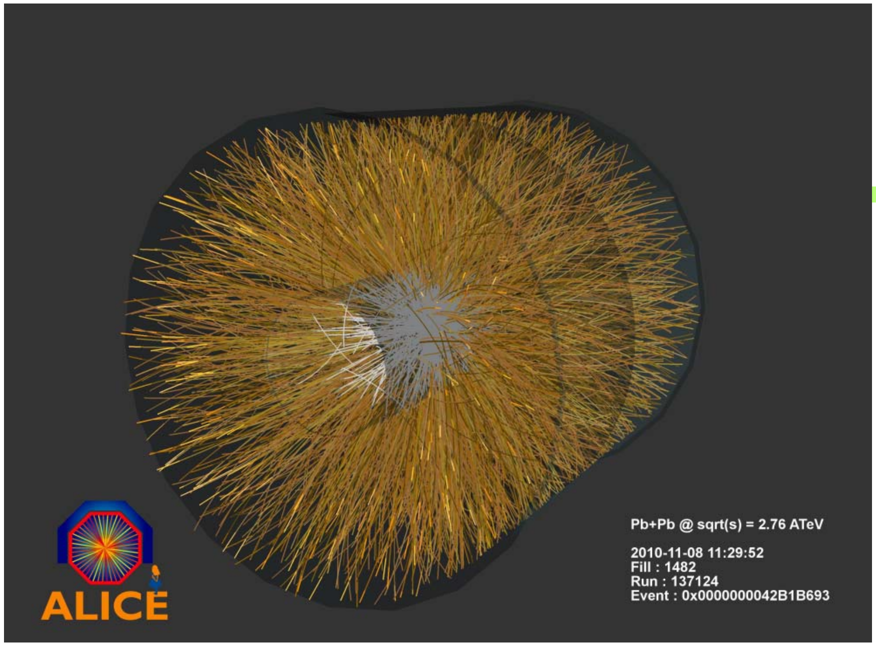

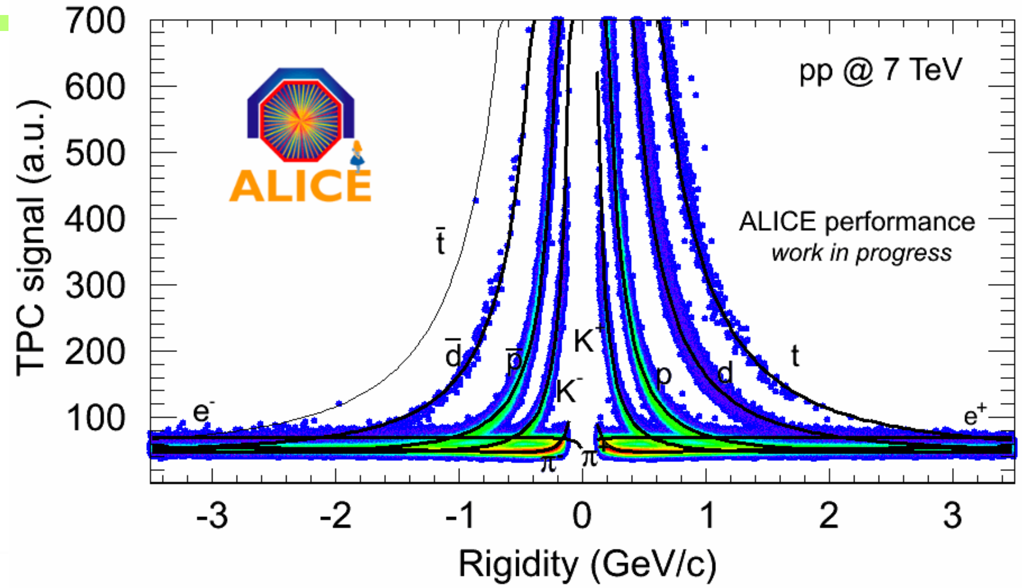

TPC dE/dx

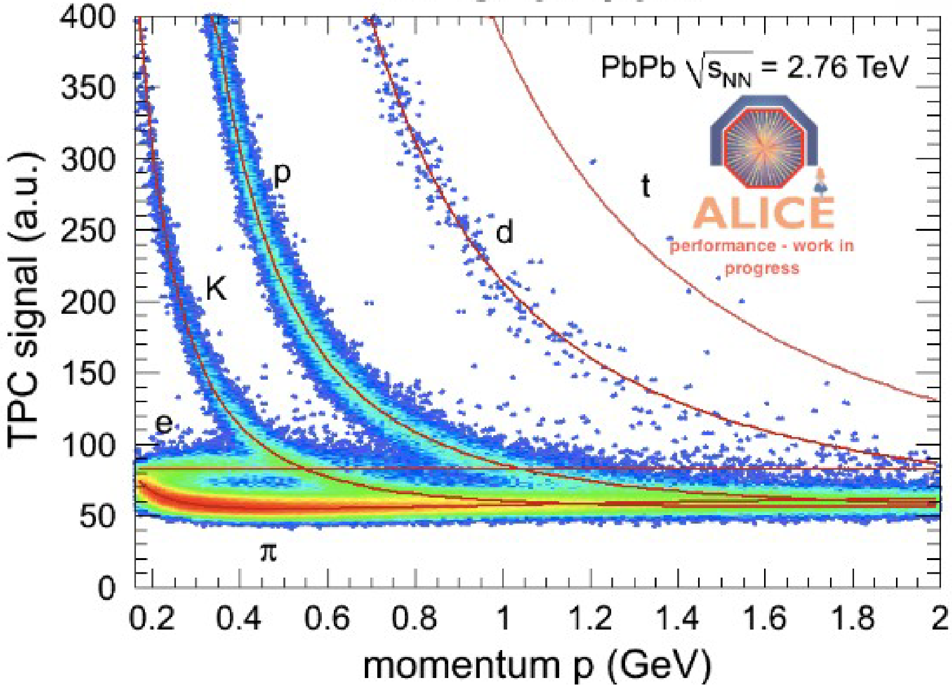

relativistic rise region

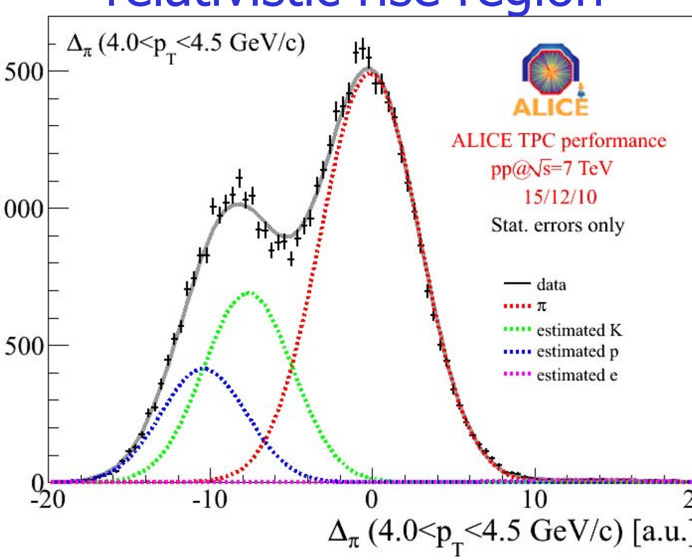

CsI based RICH counters: HADES, COMPASS, ALICE

HADES and COMPASS RICH: gas radiator + CsI photocathode – long term experience in operation

ALICE:

- liquid radiator
- proximity focusing

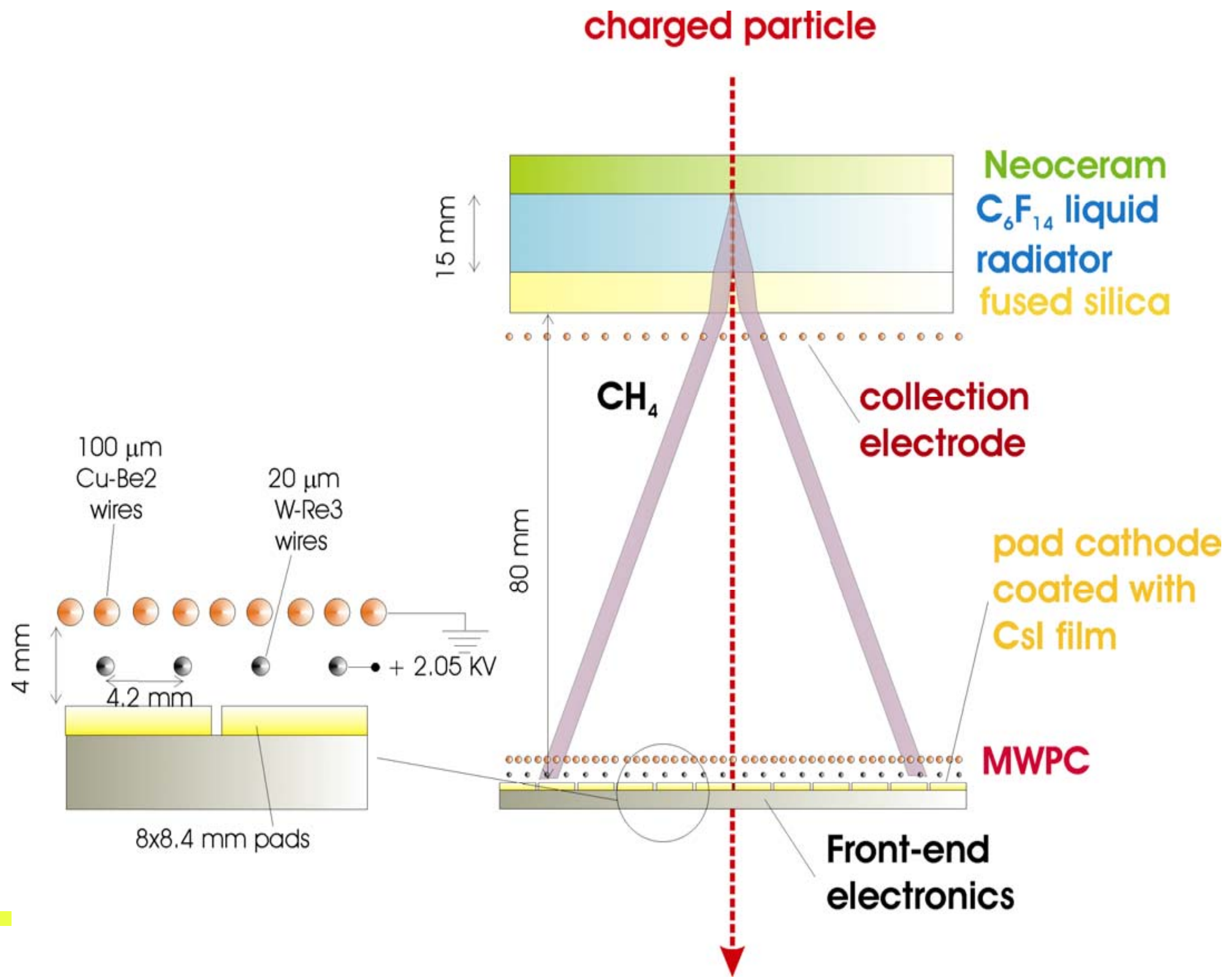

CERN CsI deposition plant

Photocathode produced with a well defined, several step procedure, with CsI vaccum deposition and subsequent heat conditioning

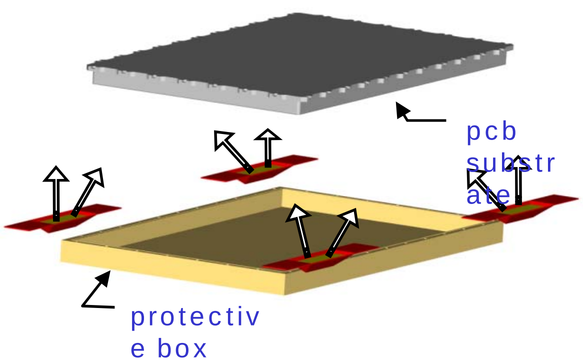

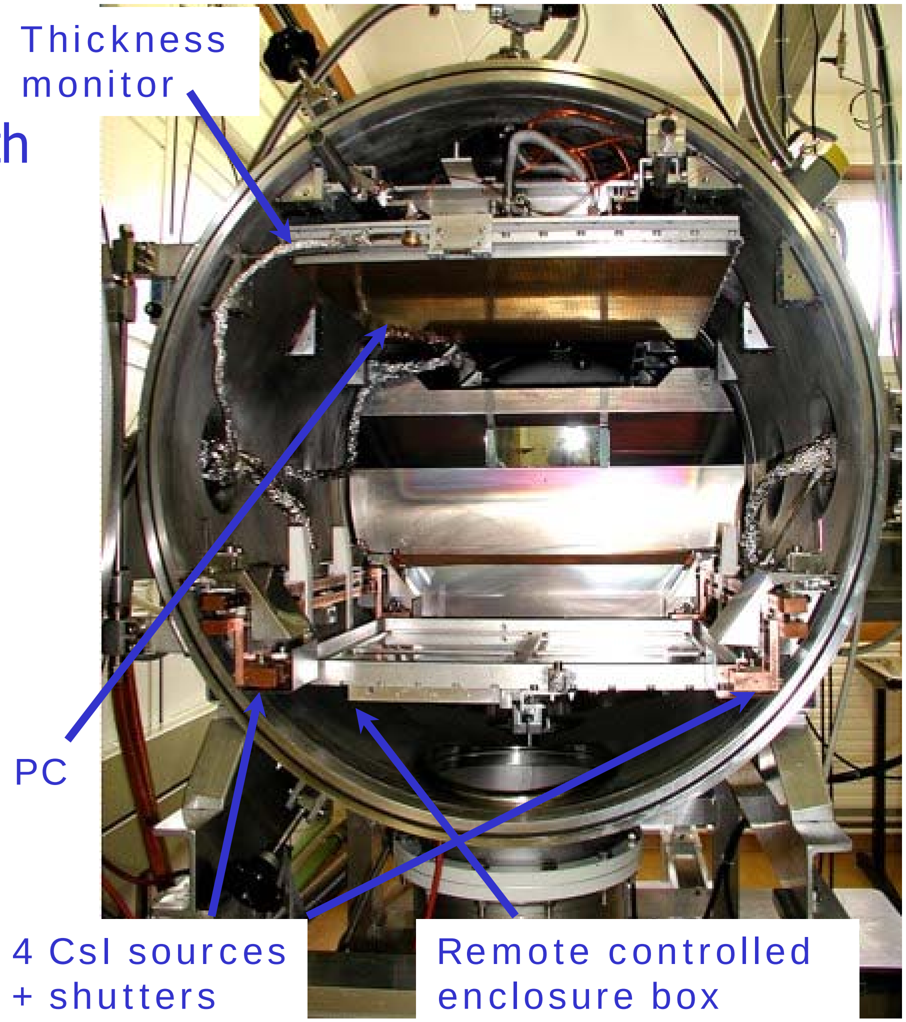

ALICE RICH = HMPID

The largest scale (11 m^2) application of CsI photo-cathodes in HEP!

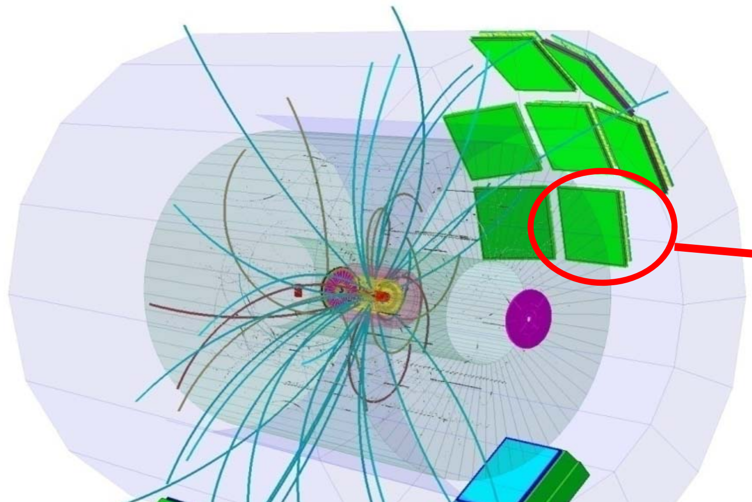

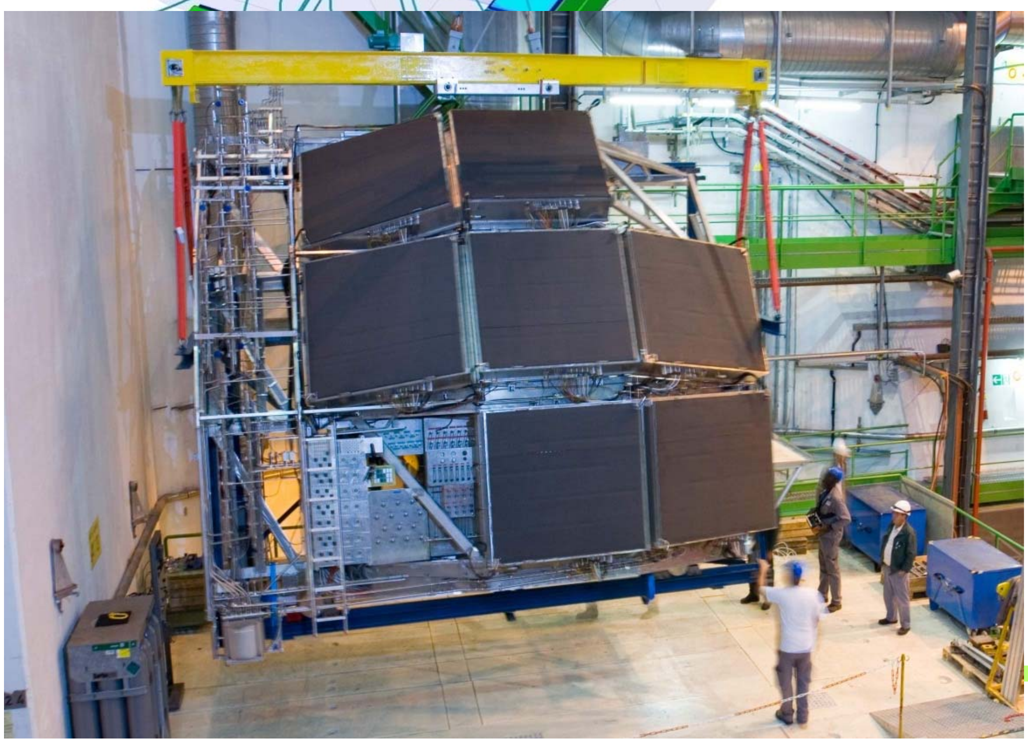

Six photo-cathodes per module

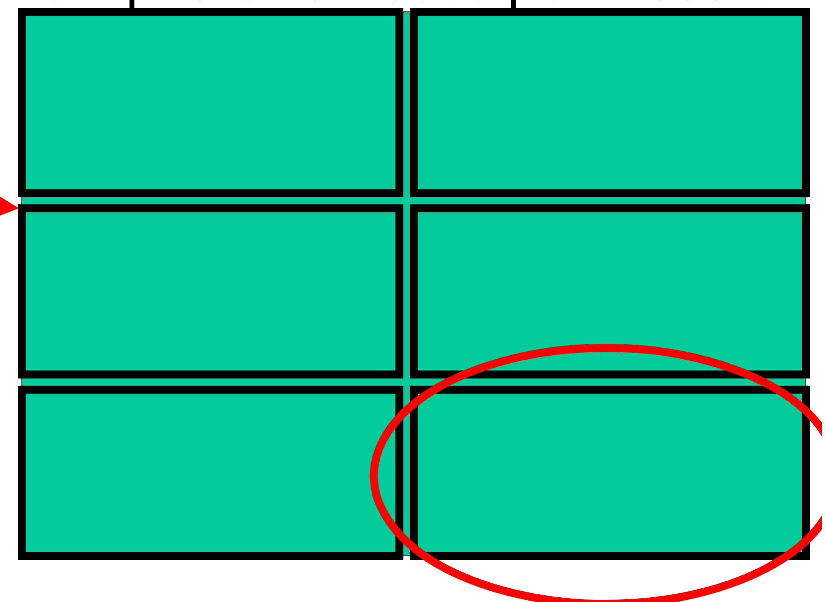

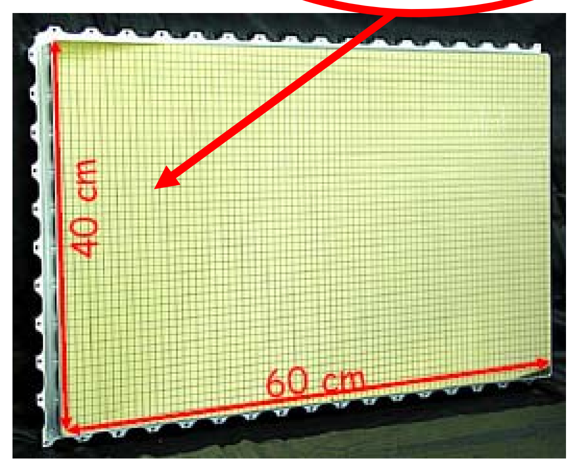

CsI photo-cathode is segmented in 0.8x0.84 cm pads

ALICE HMPID performance

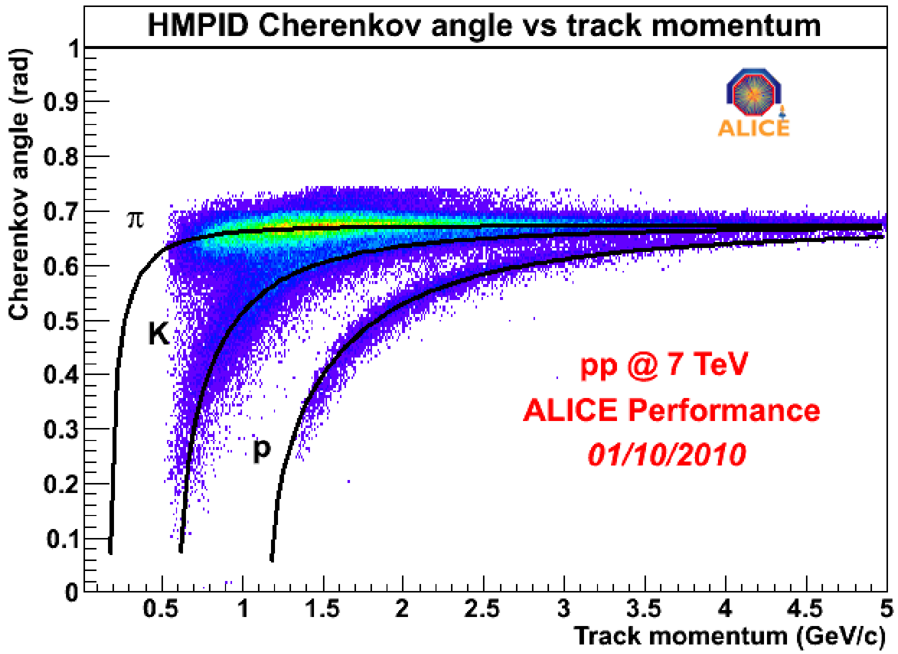

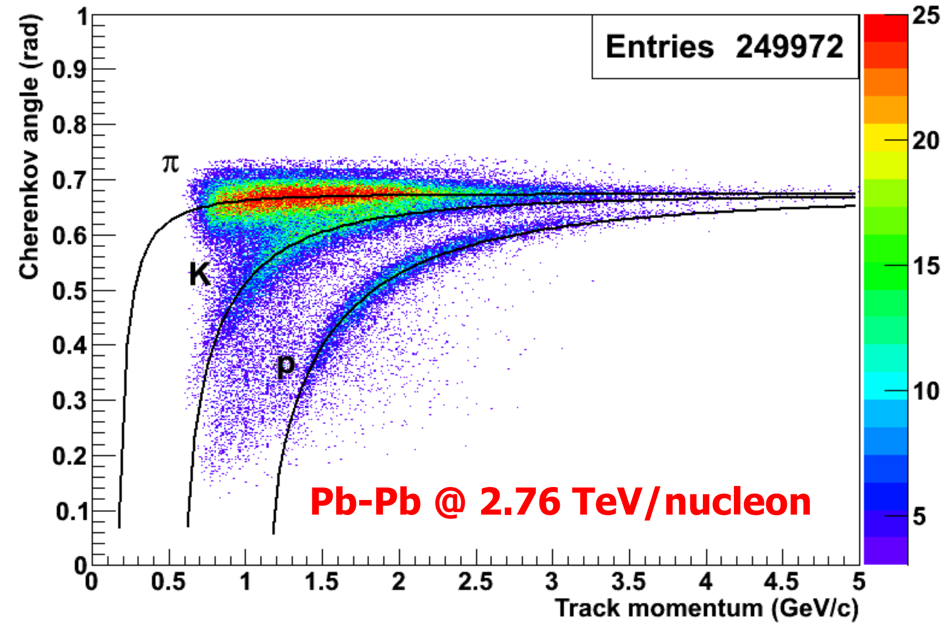

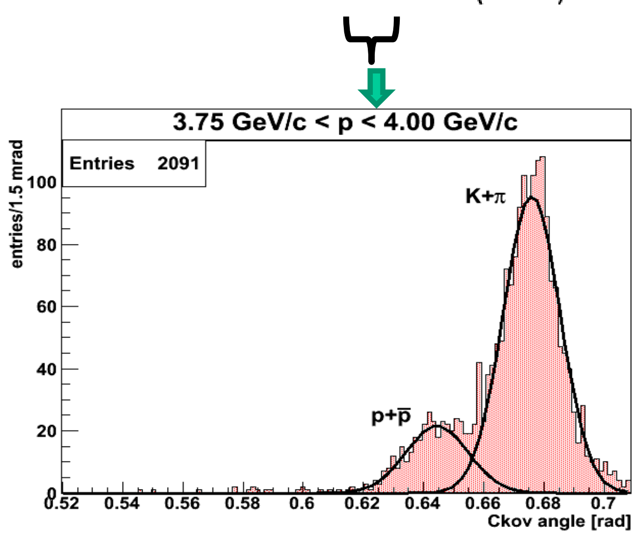

Back-up slides

TRT performance

at 90% electron efficiency

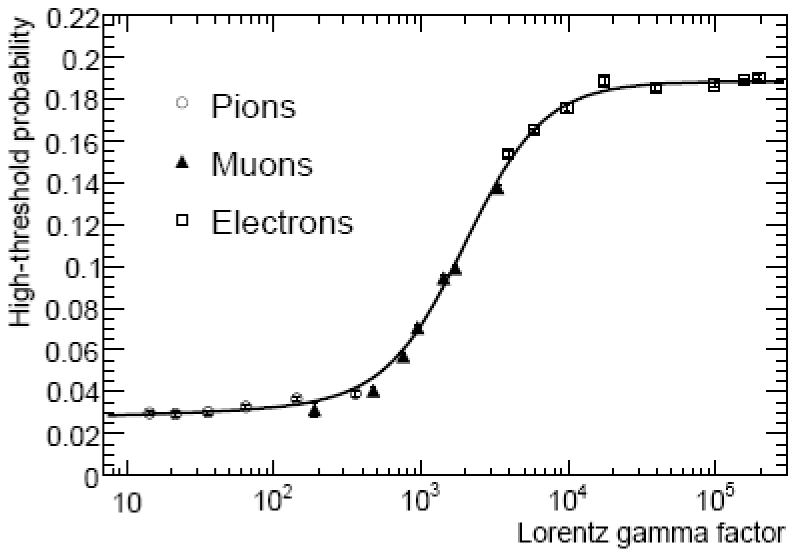

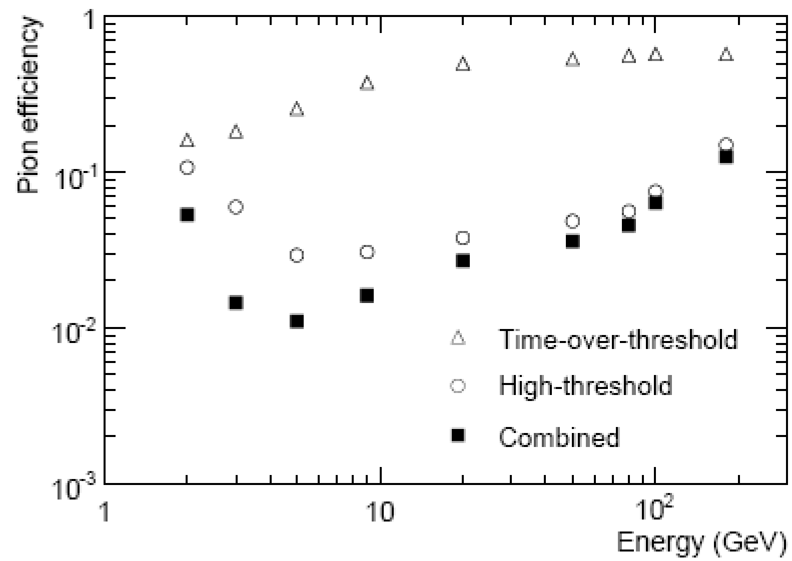

Figure 10.25: Average probability of a high-threshold hit in the barrel TRT as a function of the Lorentz γ-factor for electrons (open squares), muons (full triangles) and pions (open circles) in the energy range 2–350 GeV, as measured in the combined test-beam.

Figure 10.26: Pion efficiency shown as a function of the pion energy for 90% electron efficiency, using high-threshold hits (open circles), time-over-threshold (open triangles) and their combination (full squares), as measured in the combined test-beam.

TRT performance in 2010 data 2

dE/dx performance: time-over-threshold

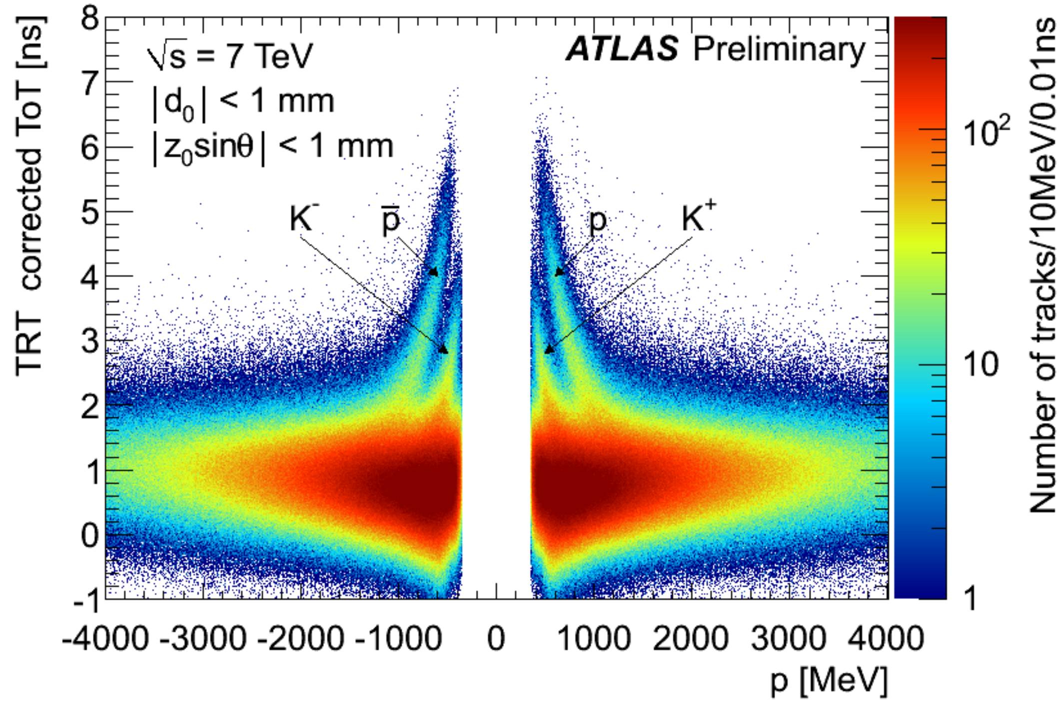

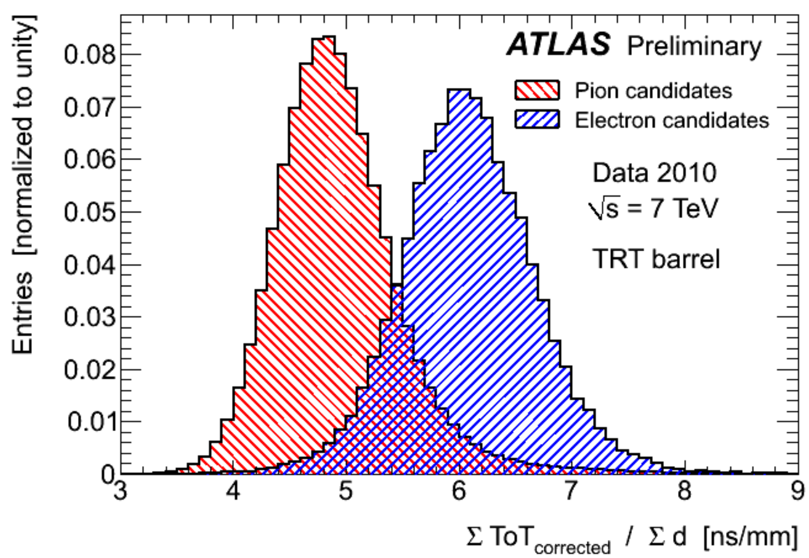

Additional e/pion separation in time-over-threshold